Journal for Nature Conservation 91 (2026) 127202

Contents lists available at ScienceDirect

Journal for Nature Conservation

journal homepage: www.elsevier.com/locate/jnc

Classification of old-growth beech forest across Europe using Sentinel-2 and airborne laser scanning

Manuela Hirschmugl [a,b,*], Carina Sobe [a], Peter Meyer [c], Hanns Kirchmeir [d], Alfredo Di Filippo [e], Ruth Vanhaecht [h], Yanitsa Ivanova [g], Kris Vandekerkhove [f]

[a] JOANNEUM RESEARCH Forschungsgesellschaft mbH, Institute for Digital Technologies, Steyrergasse 17, 8010 Graz, Austria
[b] Department of Geography and Regional Science, University of Graz, Heinrichstraße 36, 8010 Graz, Austria
[c] Nordwestdeutsche Forstliche Versuchsanstalt, Waldnaturschutz, Professor-Oelkers-Straße 6, 34346 Hann. Münden, Germany
[d] E.C.O. Institute of Ecology, Lakeside B07b, 9020 Klagenfurt, Austria
[e] DAFNE, Department of Agriculture and Forest Science, University of Tuscia, Via S.C. de Lellis, I-01100 Viterbo, Italy
[f] Research Institute for Nature and Forest (INBO), Gaverstraat 4, 9500 Geraardsbergen, Belgium
[g] Central Balkan National Park Directorate, Bodra smyana 3, 5300 Gabrovo, Bulgaria
[h] Sonian Forest Foundation, Chaussée de la Hulpe 201, 1170 Watermael-Boisfort, Belgium

ARTICLE INFO

Keywords:
Old-growth forest
Remote sensing
Airborne laser scanning
Random forest

ABSTRACT

Old-growth forests (OGF) play a critical role in biodiversity conservation and climate regulation. The preservation of Europe's remaining OGFs is therefore essential and as such addressed in the European Union's (EU's) biodiversity strategy 2030. In order to strictly protect all remaining EU primary and OGFs, their locations and extent need to be mapped. Remote sensing (RS) offers the possibility to assess extensive and remote areas. This study evaluates the use of Sentinel-2 satellite images and airborne laser scanning (ALS) data for the assessment of dominant stand age and development classes for beech forests in four test sites located in three different biogeographical regions across Europe. We use up to 150 spectral, textural and height features as input to a random forest (RF) regression. Elevation consistently ranks among the top eight most important features, showing the highest importance in mountainous regions and the lowest in predominantly flat terrain. Texture, on the other hand, varies in importance across the sites and appears to be inversely related to elevation, with higher importance values observed in flat areas. Regarding spectral indices, the Normalized Difference Red Edge (NDRE1) emerges as a significant feature across most sites. Near and short-wave infrared and the third red-edge band are important individual features in several sites. Training data is derived from existing age maps. Validation is done using 512 independent field measurement plots. The results show overall accuracies (OA) for five structural development classes between 53 and 81 % for Sentinel-2 data only. Where available, ALS data increases the OA by about 6 %. When considering only two classes (OGF vs. non-OGF), the OA is between 59 % for Bulgaria with Sentinel-2 data only and 94 % for Belgium, when including ALS. Our approach is constrained by the potential unavailability of high-quality reference data for various biogeographical regions, as well as the limited accessibility of LiDAR data. The comparison with existing global RS-based maps evidently shows many more details and higher accuracy of our products. In comparison with a European map of existing primary forests, we see overall congruence, but also differences: our approach spots similar spectral and structural characteristics in areas outside the known primary or old-growth forests. RS can thus provide valuable spatial insights into potential OGF locations to better target field visits and facilitate the faster identification of currently unprotected OGFs.

* Corresponding author.
E-mail addresses: manuela.hirschmugl@joanneum.at, manuela.hirschmugl@uni-graz.at (M. Hirschmugl), Carina.Sobe@joanneum.at (C. Sobe), peter.meyer@nw-fva.de (P. Meyer), kirchmeir@e-c-o.at (H. Kirchmeir), difilippo@unitus.it (A. Di Filippo), rvanhaecht@sonianfoundation.be (R. Vanhaecht), ivanova@centralbalkan.bg (Y. Ivanova), kris.vandekerkhove@inbo.be (K. Vandekerkhove).

https://doi.org/10.1016/j.jnc.2025.127202
Received 14 October 2025; Received in revised form 15 December 2025; Accepted 18 December 2025
Available online 23 December 2025

1. Introduction

Old-growth forests (OGFs) are forests in the late seral stages of natural forest dynamics (Leibundgut, 1982; Oliver et al., 1996), ranging from late maturity to eventual collapse. These forests are exceptionally valuable yet increasingly rare, offering a wide array of essential ecosystem services. They support biodiversity by providing habitats for a wide variety of species (Paillet et al., 2010), contribute to climate regulation and carbon sequestration (Luyssaert et al., 2008), and protect vital soil and water resources (Brockerhoff et al., 2017). Despite their importance, many old-growth forest areas remain unprotected and are threatened by legal and illegal logging (Mikoláš et al., 2023).

Given their ecological importance and their key role in many ecosystem services, the mapping and preservation of Europe's remaining OGFs are critical (Barredo et al., 2021). This priority is reflected in the EU's Biodiversity Strategy for 2030 (European Commission, 2020), which calls to identify, map and strictly protect all remaining EU's primary and old-growth forests. To facilitate this effort, a common definition for OGFs was required. The following definition was adopted within the EU strategy: *"A forest stand or area consisting of native tree species that have developed, predominantly through natural processes, structures and dynamics normally associated with late-seral developmental phases in primary or undisturbed forests of the same type. Signs of former human activities may be visible, but they are gradually disappearing or too limited to significantly disturb natural processes."* (European Commission, 2023).

Given this broad definition, two key issues must be addressed before mapping can begin. The first is the selection of indicators, as OGFs are typically not defined or identified by a single attribute (da Silva et al., 2019), but rather a combination of several factors. Various indicators can be used to define the *"structures and dynamics normally associated with late-seral development phases"* (Meyer et al., 2021). Key indicators commonly used in the literature in addition to age are: large and/or old trees (Burrascano et al., 2013; GILG, 2005; Mikoláš et al., 2019; Nilsson et al., 2003; Vandekerkhove et al., 2018; Wirth et al., 2009), standing and lying deadwood (Bauhus et al., 2009; Burrascano et al., 2013; Christensen et al., 2005; Nilsson et al., 2003), above ground biomass (Curovic et al., 2020; Meyer et al., 2021; Motta et al., 2015), diameter size and distribution (Curovic et al., 2020; Duncker et al., 2012; Ziaco et al., 2012), spatial distribution/patterns of trees and gaps (Buchwald, 2005; Rugani et al., 2013) and vertical structure (Bauhus et al., 2009; Buchwald, 2005; Martin et al., 2021; Wirth et al., 2009). The European Commission guidelines (European Commission, 2023) specify three primary indicators that must be used: native species, deadwood amounts, and old and/or large trees. In addition, at least two complementary indicators must be considered. These complementary indicators include stand origin, structural complexity, habitat trees, and indicator species. The responsibility for selecting specific indicators and determining how to measure them lies with the national authorities of the EU member state (European Commission, 2023). The second issue involves defining thresholds that distinguish OGFs from non-OGFs across various biogeographical regions and beech-dominated forest ecosystems in Europe. For example, in Western Europe, beech trees may be regarded as 'old' or 'overmature' at around 150 years, whereas in the Carpathians, this distinction typically applies to trees that are at least 200 years old. Transparency, as emphasized by the guidelines, is crucial, but these regional variations make a pan-European mapping approach particularly challenging. Within the LIFE + PROGNOSES project a catalogue of criteria and indicators for beech OGFs has been developed. The seven criteria include: presence of (large and) old trees, quantity and quality of lying and standing deadwood, structural diversity of living stand, tree species composition, soil microstructures (micro-relief), tree microstructures, and presence of indicator species. In this study, we focus on one of the keys and relatively operational indicators: stand age and development classes, which serve as an indirect proxy for the structural characteristics of OGFs. The threshold value for beech OGFs was set to 150 years (Vandekerkhove et al., 2022) aligning with recommendations from the German Scientific Advisory Board (Scientific Advisory Board on Forest Policy, 2023). It is important to note that this threshold selection may result in larger OGF areas being identified in Eastern Europe than previously expected or reported in other studies. Additionally, we emphasize that old trees are not necessarily large, as their size is influenced by local growth conditions. For this reason, age values are used in this study as the primary criterion for identifying beech OGFs.

The current state-of-the-art in OGF mapping in Europe can be divided according to the main source of information. This information can come from field inventories (Meyer et al., 2021), historical maps (Grabska-Szwagrzyk et al., 2024) and long-term land use records (Munteanu et al., 2021), expert-compiled inventories (Sabatini et al., 2021), existing data bases (Barredo et al., 2021), and from RS. Within the group of RS-based methods, three different approaches can be distinguished (Hirschmugl et al., 2023b): parameter-based approaches, direct and indirect approaches. Regional mapping exist for example covering the Ukrainian Carpathians (Spracklen and Spracklen, 2019) or the Bavarian Forest National Park in Germany (Adiningrat et al., 2024). Despite these advancements, a significant knowledge gap remains between existing data and methods and a comprehensive European-wide map of OGFs. Furthermore, there is a lack of operational mapping methods and robust validation techniques for large areas. The objectives of this study are twofold: first, to develop an RS-based mapping approach for estimating forest stand age and assessing the associated structural development classes as a key parameter for identifying beech OGFs in different biogeographical regions across Europe (Roekaerts, 2002); and, second, to implement a scientifically sound accuracy assessment to validate the results. This accuracy assessment is based on homogeneous field measurements generated within the LIFE + PROGNOSES project, completely independent from the used training data. In terms of applications, the main aim is to support the European Forestry Policy by providing a methodology for identification of potentially OGF areas. These areas can further be used for targeted field surveys to identify and map all OGFs in Europe (European Commission, 2020) or as ideal candidates for stepping stones in processes related to the Nature Restoration Law (European Commission, 2024).

The intrinsic challenges of conducting a European-wide, RS-based assessment of primary and old-growth forests are threefold: first, the different characteristics of beech OGF in different biogeographical regions; second, discrepancies in the timing and quality of available training and validation data; and third, the diverse types and quality of remote sensing data available across Europe. This study aims to address these challenges by exploring the following research questions:

(1) Is there a one-size-fits-it-all methodology for identifying potential old-growth beech forests across Europe?
(2) What is the achievable accuracy for classifying structural development classes of beech forests from RS data, validated with independent field-measured plot data?
(3) What is the benefit of incorporating airborne laser scanning (ALS) data into this classification process?

2. Materials and methods

2.1. Test sites

The test sites used in this study were selected from those covered by the LIFE + PROGNOSES project, primarily due to the harmonized field data collection methodology employed for validation during the accuracy assessment. Fig. 1 provides an overview of the four test sites, which are distributed across Europe and represent different biogeographical regions. These sites include: (1) the Sonian Forest (SOFO) in Belgium, (2) the National Park Kalkalpen (NPKA) in Austria, (3) the Abruzzo National Park (ABNP) in Italy, and (4) the Central Balkan National Park

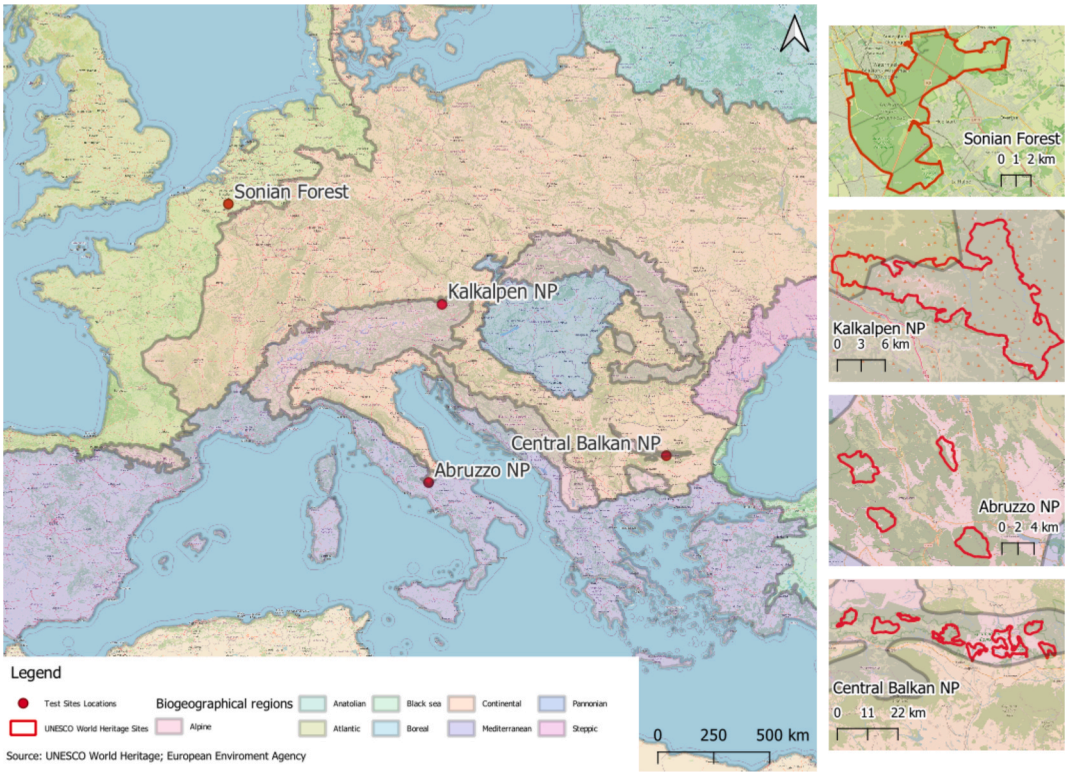

Fig. 1. Overview of the test sites (Sources: UNESCO World Heritage Sites; Biogeographical regions of Europe: https://data.europa.eu/).

(CBNP) in Bulgaria. The national parks (or portions thereof) shown on the left side of Fig. 1 are part of the UNESCO World Heritage sites 'Ancient and Primeval Beech Forests of the Carpathians and Other Regions of Europe' (Kirchmeir and Kovarovic, 2016).

Covering an area of over 4000 ha, SOFO in Belgium is dominated by beech forests originating from managed stands, and with stand ages ranging up to 250 years. For this study, we selected a sub-area of about 1000 ha, which includes the full age range and a World Heritage component of about 230 ha of set-aside old beech forest (Vandekerkhove et al., 2018). SOFO is part of the Atlantic beech forest region and ranges from 65 to 130 m in altitude above sea level. The second site, NPKA in Austria, encompasses 5251 ha, with altitudes ranging from 396 to 1963 m. Many trees here are over 140 years old, forming part of the alpine beech forest region and representing one of the largest primeval beech forests in the Alpine region (Mayrhofer et al., 2015). The third site is a subset of about 936 ha within the Abruzzo, Lazio and Molise National Park in Italy, situated at an altitude of 1400–1850 m. The site includes several proven trees that are over 586 years old (Piovesan et al., 2003). The largest test site is CBNP in Bulgaria, covering an area of 10,988 ha. The site features diverse forest habitats, including Middle European dry-slope limestone beech forests and Balkan Range bedstraw beech forests (Nikolov and Dimitrov, 2023).

2.2. Data

The methodology applied in this study is based on a combination of remote sensing and field data. The remote sensing data (see Section 2.2.1) includes Sentinel-2 satellite data (Drusch et al., 2012), the Shuttle Radar Topography Mission Digital Elevation Model (SRTM-DEM) and ALS data. Field data consists of polygon-based training data of various origins (see Section 2.2.2) and plot-wise, field-based validation data (see Section 2.2.3) collected as part of the LIFE + PROGNOSES project. By integrating satellite imagery, laser scanning data, and field data, this approach enables a comprehensive analysis and identification of forest structure. Furthermore, the inclusion of validation data ensures the accuracy and reliability of the results.

2.2.1. Remote sensing data

This study utilizes three types of remote sensing data: optical satellite imagery from the Sentinel-2 satellites, digital elevation data from the Shuttle Radar Topography Mission (SRTM), and airborne laser scanning (ALS) data, which is available for two of the test sites only. The Sentinel-2 mission currently consists of three satellites equipped with basically identical multispectral sensors. These satellites map every point on Earth at least every five days at an average altitude of 786 km, capturing data across 13 spectral bands (Drusch et al., 2012). Four of these bands – red, green, blue, and near-infrared – are captured at a spatial resolution of 10 m. Six additional bands, including vegetation red edge and short-wave infrared (SWIR) bands, are captured at 20 m resolution. The remaining three bands, dedicated to atmospheric observations, are captured at 60 m resolution (Drusch et al., 2012), however, these were not used in this study. Since 2022, a standardized pre-processing framework for Sentinel-2 data with varying processing levels has been established (European Space Agency, 2015). In this study, Level 2A data was used for processing all temporal statistics and indices, while Level 1C data was utilized exclusively for cloud masking.

Sentinel-2 data from May to October was selected to avoid snow and leaf-off conditions during the winter months. For NPKA, SOFO and ABNP Sentinel-2 data from 2018 was used. For NPKA and SOFO, this year was chosen as the closest available data to the ALS data acquisition dates (2018 in NPKA; 2014 in SOFO). For CBNP, Sentinel-2 data from 2022 was utilized due to the poor quality and high cloud cover in the 2018 Sentinel-2 data, as well as the absence of ALS data for comparison.

The second type of RS data used in this study is ALS data, which provides detailed information not only about the canopy surface but also penetrates the crowns to deliver insights into tree heights and forest structure. ALS data is available for portions of the SOFO and NPKA test sites. For SOFO, the data was collected in 2014 using a Riegl LMS-Q6801

sensor, with a minimum point density of 16 points per square meter (Digitaal Vlaanderen, 2023). For NPKA, ALS data was acquired in 2018 using a RIEGL VQ-580 sensor mounted on an aircraft flying at an altitude of approximately 790 m, achieving a point density of more than 16 points per square meter (Hirschmugl et al., 2023a). The third RS dataset used in this study is the Shuttle Radar Topography Mission (SRTM) Digital Elevation Model (DEM), a global dataset that provides terrain elevation information for the Earth's surface. This data was derived from radar interferometry collected during an 11-day mission in February 2000 (Farr et al., 2007).

2.2.2. Field data

The field data utilized in this study consists of two components: reference data and validation data. The reference data, provided as polygon shapefiles, form the foundation for training the classification model. These data were compiled through a combination of historical forest inventory maps, in situ field assessments, and expert interpretation of aerial imagery. While the specifics of the training data vary across the four study sites, polygon-based average stand age information was consistently available for all sites, ensuring uniformity in model training. Additionally, the reference dataset includes information on tree species composition, which is particularly relevant given the study's focus on beech-dominated forests.

Independent validation data were employed to ensure robust model performance assessment. This step is crucial when using remote sensing data in conjunction with machine learning algorithms such as the Random Forest (RF) regressor (Belgiu and Drăguţ, 2016). Independent validation not only facilitates an objective evaluation of model accuracy but also mitigates the risk of overfitting. This allows for a real-world accuracy estimation, while the standard training-test-validation data split is often biased (Xu and Goodacre, 2018). The validation data consists of field plots evaluated as part of the LIFE PROGNOSES project. These field mapping areas were selected based on criteria such as the proportion of beech and other tree species, stand age, degree of management, and canopy cover (Kirchmeir et al., 2023). Most of the field data is freely available, with all details on data, sites, and methods published (Vanhellemont, 2025). The main goal of this mapping effort was to create a standardized approach to data generation across Europe using a common mapping guideline (Kirchmeir et al., 2023). Since the test sites are chosen to cover a wide range of environmental conditions and land use patterns, it is crucial that the validation process is comparable across all sites. In terms of age, it is easier to determine the age of a tree than the age of a forest plot, as the plot can contain young and old trees at the same time. In contrast, our RS-based mapping does not allow determination of individual tree age due to (a) the resolution of the Sentinel-2 data covering potentially (parts of) several trees and (b) the structure of the stand, which contributes to spectral signal of the Sentinel pixels as much as the spectral reflectance of the leaves themselves (Adiningrat et al., 2024). To address these challenges, the original age classes listed in Table 1 were consolidated into five final structural development classes with comparable age limits. It is worth clarifying that these limits represent a compromise between the recommendations of the LIFE PROGNOSES project, existing guidelines, and the practical resolution constraints of the RS data. However, it ensures consistency and facilitates meaningful comparisons across the study sites.

Table 1
Development classes assigned to the plots during field inspection.

Original age class	Merged structural development classes	Explanation
Very young managed	initial phase (IP)	even-aged clearcut/regeneration stage (0–10 yr)
Young natural		rejuvenation/initial phase or young growth (0–10 yr)
Young managed	pole/stem exclusion phase (EP)	even-aged young growth dense stands up to pole wood (10–30 yr)
Intermediate managed	aggradation phase (AP)	even-aged young timber / stem exclusion phase (30–60 yr)
Natural aggradation		natural aggradation phase
Even-aged mature stand	mature and mixed developmental phase (MP)	dominant trees 60–150 yr old
Uneven-aged		containing all ages, young up to mature, in Plenterwald
Two-aged		shelterwood, coppice-with-standards
Even-aged overmature	late-seral/overmature phase (OP)	even-aged overmature stand (dominant trees > 150 yrs)
'Set aside', overmature		uneven-aged overmature (dominant trees > 150 yrs)
Natural overmature		late-seral/overmature phase (dominant trees > 150 yrs old)
Natural senescence		senescence/decaying phase (collapse of the dominant trees) (remaining standing trees > 150 yrs old)

2.3. Methods

The overall technical workflow is depicted in Fig. 2 and used for all test sites. In the subsections below, each step is individually explained.

2.3.1. Standardized pre-processing of RS data

This section outlines the pre-processing steps for RS data and the calculation of input features. Sentinel-2 Level 1C data (ESA, 2023) was used to generate cloud masks, which were applied to Level 2A data for each image acquisition during the observation period. For each test site, 10 spectral bands (10 m and 20 m resolution) were utilized to calculate temporal features, indices, and texture features. The selected indices, based on existing literature, include the Normalized Difference Vegetation Index (NDVI), Tasseled Cap Greenness (TCG), BrightnessRGB, Green Normalized Difference Vegetation Index (GNDVI), and Normalized Difference Red Edge 1 (NDRE1). NDVI, derived from red and near-infrared bands, is widely used for environmental monitoring (Rouse et al., 1974) and has proven effective for identifying old-growth forests (Boiarskii, 2019; Laurin et al., 2017; Spracklen and Spracklen, 2019). TCG is commonly applied for vegetation mapping, detecting large-scale forest disturbances, and assessing vegetation density and dynamics (Czerwinski et al., 2014; Healey et al., 2005; Jin and Sader, 2005). Small-scale forest disturbances and related irregular vegetation density are typical patterns in OGFs. BrightnessRGB, based on red, green, and blue bands, provides insights into chlorophyll content (Ciocîrlan et al., 2022). GNDVI serves as an indicator of plant vigor and also for chlorophyll levels (Espinoza et al., 2017). Finally, NDRE1, which uses the first red edge band, is useful for monitoring plant chlorophyll and identifying nitrogen-deficient areas (Boiarskii, 2019; Carlson and Ripley, 1997). The relationship between forest maturity and chlorophyll content is complex and depends on several factors, including species composition, canopy structure, forest health, and environmental conditions. OGFs typically feature complex, multi-layered canopies with gaps and varying light availability, which affects chlorophyll content across different layers. This structural complexity, combined with established nutrient cycling in mature trees, often results in moderate but more stable overall chlorophyll levels compared to younger forests with vigorous growth. Additionally, chlorophyll levels can reflect a forest's resilience and stability, distinguishing OGFs from disturbed or managed forests. While chlorophyll content alone does not directly define an OGF, it serves as a valuable proxy for assessing vegetation health, canopy dynamics, and forest structure - key characteristics of OGFs.

For all Sentinel-2 bands and indices, the following temporal statistics were calculated for the vegetation period: median, 10th percentile (Perc_10), 90th percentile (Perc_90), and standard deviation (STD). This process resulted in 60 input features (10 bands plus 5 indices, totaling 15 variables, each multiplied by 4 temporal statistics). Additionally, the SRTM-DEM was also included to estimate height above sea level,

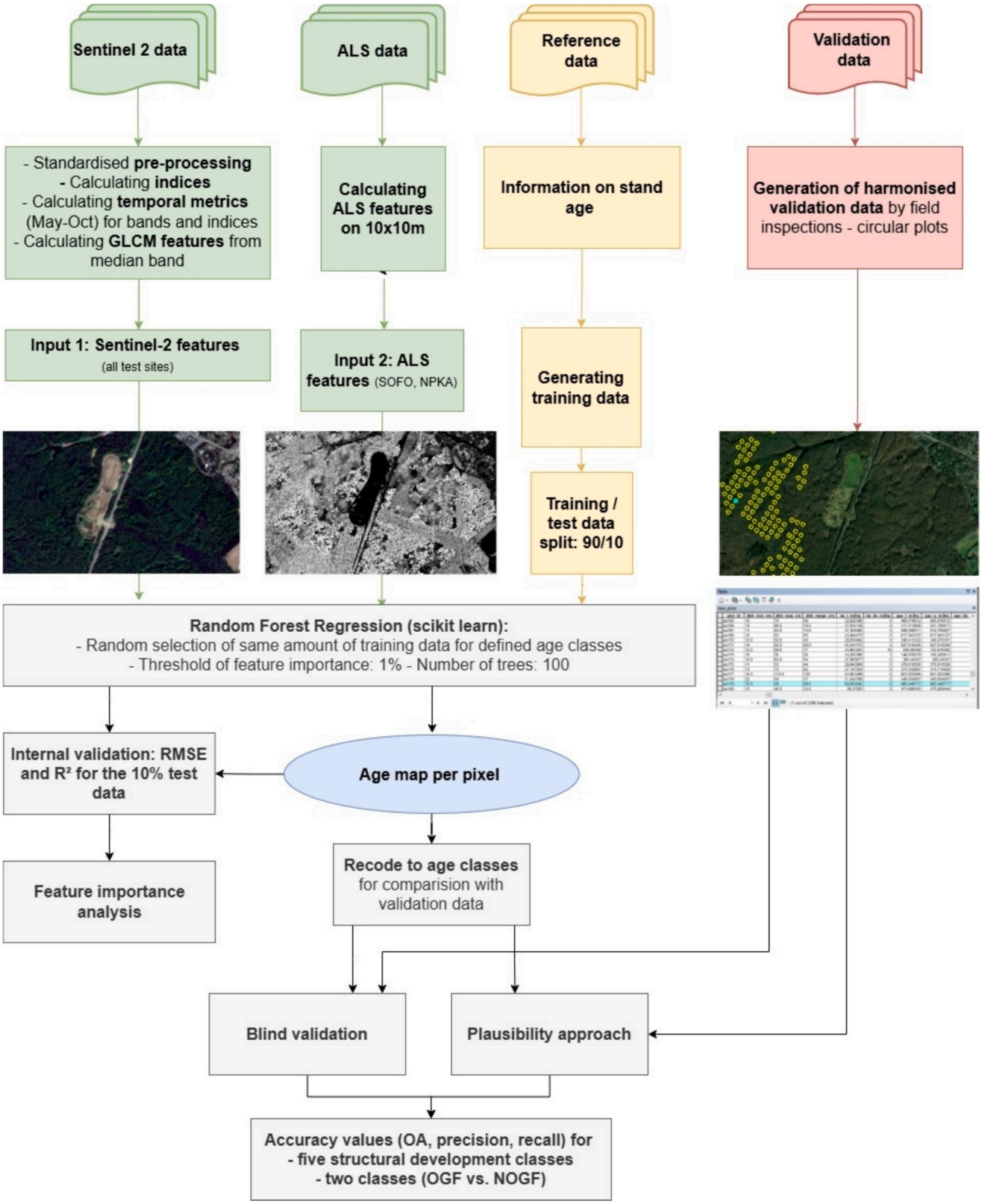

Fig. 2. Workflow diagram.

particularly for regression estimations and areas without ALS data. Spatial variability, which is known to correlate with stand development (Cohen et al., 1995) was measured using Haralick texture features (Haralick et al., 1973), also referred to as gray level co-occurrence matrix (GLCM) features. GLCM features were calculated based on the median of each spectral band within a 3 × 3 moving window. Previous studies (Adiningrat et al., 2024) have demonstrated the efficiency of specific GLCM bands – such as mean, variance, homogeneity, contrast, dissimilarity, entropy, second moment, sum average, and correlation – in age classification. Unlike Adiningrat et al. (2024), who calculated

GLCM features from a single selected image, we calculated GLCM features based on the median of the vegetation period. Using the median reduces the influence of residual clouds or artifacts from individual images, thereby improving the reproducibility and robustness of the results.

For ALS, the following parameters were processed for usage in the RF regression: maximum vegetation height, mean vegetation height, standard deviation of mean vegetation height, tree density (derived from tree top detections using a raster-based, multi-scale Laplacian-of-Gauss local maximum approach, similar to (Monnet et al., 2010)), curvature range of canopy (Griffith et al., 2015), canopy cover, elevation (mean height above sea level), terrain slope, and foliage height diversity index (Hirschmugl et al., 2023a; MacArthur and MacArthur, 1961) derived from the point cloud. All ALS parameters were calculated on the same 10 × 10m grid as the Sentinel-2 images. All input RS data sets and features are listed in Table 2, a detailed list of abbreviations and descriptions is provided in Annex 1. For SOFO and NPKA, both sets of input data (with and without ALS data) are used separately to study the effect of including ALS data in the classification.

2.3.2. Reference data preprocessing for training

For training, the polygon shapefiles with stand age information were used to develop the regression model. There is no information on the quality of the training data, as they stem from a combination of field data, visual interpretation and extrapolation of old management or reference maps. However, training areas are essential for supervised machine learning algorithms. To minimize the effects of potential errors in the training data, the polygon data were converted into individual points according to the raster grid (10 × 10m) of the Sentinel-2 data. In order to provide the classifier with an even number of training samples for different ages, classes of 20 years were defined for the selection of the training points. 2000 points were randomly selected from each 20-year age class but still retaining the original age information (not the 20-year average value). As ALS data are only available for a small section of the entire SOFO and NPKA study area, those of the 2000 selected points that lie within the smaller section were used for calculating the regression model for the combination of Sentinel-2 and ALS data. The selected training points were then split using the 90/10 separation. 90 % of the training data is used for training the algorithm, 10 % is used to determine the root mean square error (RMSE) and the coefficient of determination (R^2) in the model performance validation.

Table 2
Remote sensing input data.

Data	Bands	Input features for model estimation	Nr. of features
Sentinel-2 time series data (SOFO, NPKA, ABNP: may–october 2018; CBNP: may–october 2022)	**Spectral bands:** B2, B3, B4, B5, B6, B7, B8, B8A, B10, B11	Four temporal statistics: median, standard deviation, 10th percentile (Perc_10), 90th percentile (Perc_90)	40
	Vegetation indices: BrightnessRGB, GNDVI, NDVI, NDRE1, Tasseled Cap Greenness (TCG)		20
	GLCM texture features (calculated from temporal median band): B2, B3, B4, B5, B6, B7, B8, B8A, B10, B11	Angular Secondary Moment (ASM), Contrast, Correlation, Dissimilarity, Entropy, Homogeneity, Mean, Sum Average, Variance	90
ALS data (SOFO: 2014; NPKA: 2018)	standard features	maximum vegetation height (Max_Veg_Height), mean vegetation height (Mean_Veg_Height), tree density, mean height above sea level (Elevation), terrain slope	9
	structural features	curvature range of canopy, canopy cover, standard deviation of vegetation height, foliage height diversity	
SRTM DEM		Digital elevation model height above sea level (DEM)	1

2.3.3. Random forest regression

For the regression model, Random Forest (RF) regression was employed. RF regression shares a similar structure with the RF classifier, consisting of multiple tree-structured models. However, it focuses on predicting continuous variables rather than class labels. In regression, random feature selection is applied alongside bagging, while out-of-bag estimation is used to monitor error and assess variable importance. The algorithm aims to minimize residual correlation and employs randomization to reduce average error, contrasting with the classification approach, which aggregates votes for the most popular class (Breiman, 2001). To better understand the contribution of individual features in RF regression, a feature analysis was conducted. This analysis evaluates the impact of input data on the model, identifying which features are most important and how much they contribute to the outcome. By doing so, the complex structure of the model becomes more transparent, facilitating its application to different use cases or test sites (Rengasamy et al., 2022). Feature importance was calculated using Gini Importance, which measures the significance of a feature in reducing Gini impurity – a metric for data homogeneity (Menze et al., 2009). We used 1 % as threshold for features (Prasetiyowati et al., 2021; Sobe et al., 2021) meaning that all features exceeding this threshold were included in the regression. The Random Forest (RF) regression implementation used in this study is from scikit-learn (sklearn.ensemble.RandomForestRegressor). The dataset was split into 90 % training data, which was used to build the RF regression model, and 10 % test data for model validation. Within the sklearn RF regression, the entire 90 % training data were utulized for parameter tuning (*bootstrap = true, max_samples = none*). Regarding the model settings, 300 trees (*n_estimators = 300)* were used, and the minimum number of samples required to be at a leaf node was set to 1 (*min_samples_leaf = 1*). All other parameters were kept at their default values *(criterion = squared_error, max_depth = none, min_samples_split = 2, min_weight_fraction_leaf = 0.0, max_features = 1.0, max_leaf_nodes = none, min_impurity_decrease = 0.0, oob_score = false, n_jobs = none, random_state = none, verbose = 0, warm_start = false, ccp_alpha=0.0, monotonic_cst = none)*. The RF regression was performed in two stages: the first run was trained using all input features. Feature importance was then calculated for each feature based on this initial run. Only features with a feature importance exceeding the threshold of 1 % were used for training in the second run. This two-stage approach helps to generalize the RF regression estimator and reduces the risk of overfitting. The predicted values from the second run were compared to the reference values from the 10 % test data (not used in training) to calculate RMSE and R^2.

The output of the RF regression model is an estimated forest age per pixel (in years). To compare these pixel values with the development

Table 3
Translation values between classified age and assigned structural development classes.

Code	Merged structural development classes	Age classification thresholds
IP	initial phase	≤ 10 years
EP	pole/stem exclusion phase	$30 \leq x > 10$
AP	aggradation phase	$60 \leq x > 30$
MP	mature and mixed developmental phase	$150 \leq x > 60$
OP	late-seral/overmature phase	$x > 150$

classes assigned in the field, the estimated ages were reclassified into the development classes defined in Table 1. For example, the initial phase (IP) was assigned to pixel values ≤10 years, all threshold values for reclassification are provided in Table 3.

2.3.4. Accuracy assessment

Two approaches were used for the accuracy assessment: model accuracy assessment and independent field validation. The first approach evaluates the model's accuracy by comparing predicted values with a percentage set aside of the training data as explained in the methods section. Output values of this model accuracy assessment are the RMSE and an R2 based on the 10 % test data set aside from the training data set.

The second approach assesses accuracy using completely independent field data. Field-assessed development classes were transformed into the five target structural development classes (see Table 1). Similarly, pixel-based age information from the RF regression was reclassified into these five development classes (see Section 2.3.3). In the first step – blind validation – the field plot positions were directly compared to the corresponding pixel values at the same coordinates. Standard accuracy metrics, such as overall accuracy (OA), recall, and precision, were calculated. Slight geolocation errors, which easily occur during field inspection, can jeopardize the result. However, slight geolocation errors, which are common during field inspections, can affect results, particularly in forested and mountainous areas. Such errors are known to be especially pronounced in broadleaf forests (Feng et al., 2021) with some authors noting that handheld receivers are often unsuitable for precise plot establishment due to their inaccuracy (Valbuena et al., 2010).

To address this issue, a plausibility approach was applied in the second step. Spatial inconsistencies between classified pixel values and field reference data were systematically assessed using a shifting algorithm. For each field plot, the surrounding neighborhood within a 5 × 5 pixel window (25 m in each direction) was scanned to identify nearby pixels matching the reference class. This buffer size aligns with previous findings on handheld GNSS receiver accuracy (McRoberts, 2010; Strunk

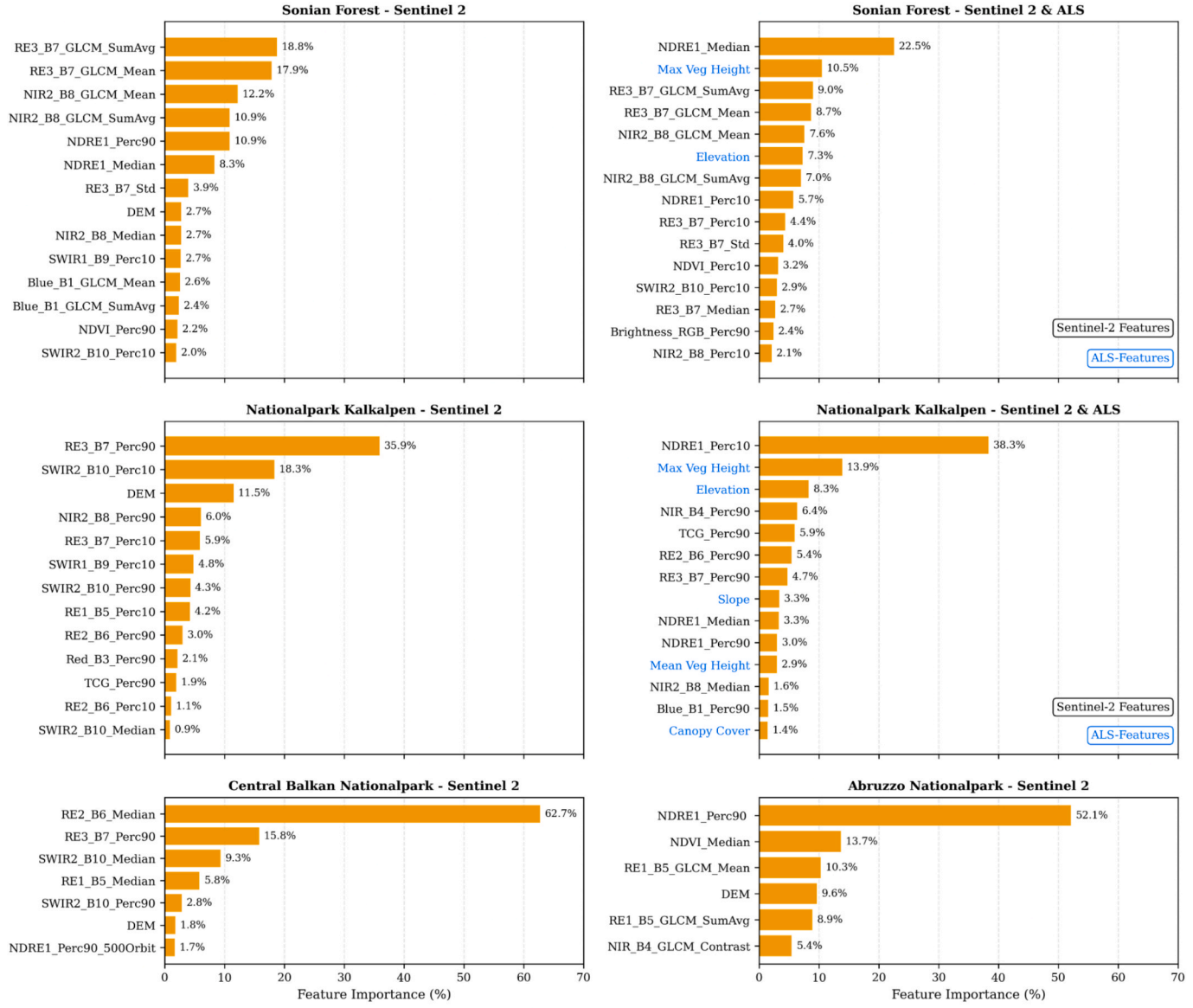

Fig. 3. Results of the feature importance analysis. S2 feature names were constructed according to the following pattern: [Spectral Feature]_[Band ID]_[Method] [Metric]. For instance, the variable RE3_B7_GLCM_SumAvg refers to the GLCM Sum of Averages texture feature, calculated on Sentinel-2 Band 7, which corresponds to the third red edge band (RE3). (B1 = Blue, B2 = Green, B3 = Red, B4 = NIR, B5 = RE1, B6 = RE2, B7 = RE3, B8 = NIR2, B9 = SWIR1, B10 = SWIR2) More details on abbreviations see Annex 1. (For interpretation of the references to colour in this figure legend, the reader is referred to the web version of this article.)

et al., 2025). If a suitable pixel was found, the plot location was virtually shifted to that position, and both distance and direction (aspect) of the shift were recorded. OA, recall and precision were then recalculated. This method quantified the proportion of classification discrepancies that could plausibly be attributed to minor spatial misalignments rather than model error, providing a refined interpretation of classification accuracy.

3. Results

3.1. Input feature importance

The results of the feature importance analysis are presented in Fig. 3. It is important to note that there was no restriction on the number of features included; all features exceeding the feature importance threshold were considered. Consequently, the number of features used varied across different sites and settings, as illustrated in Fig. 3.

Among the features, elevation (or DEM in cases without ALS data) was consistently ranked within the top eight most important variables across all sites. As anticipated, its influence was lowest in SOFO, which is characterized by relatively flat terrain (ranked 8 and 6, respectively). However, elevation played a more significant role in mountainous sites, ranking 6th for CBNP, 4th for ABNP, and 3rd in both NPKA settings. In contrast, Sentinel-2 texture metrics were highly ranked for SOFO (occupying all top three ranks for SOFO and rank 3 for SOFO_ALS) and ABNP (ranks 3, 5, and 6). This suggests that texture metrics are not equally important across all biogeographical regions and topographic contexts.

Regarding spectral features, no clear model preference was observed across all sites. However, NDRE1 statistics (10th percentile, 90th percentile, mean, and median) consistently ranked high in all cases except for NPKA (S2 only). Fig. 4 presents the relative frequency of all spectral bands and indices in a spider chart. Among individual bands, NIR2 (20 m NIR band), SWIR2, and RE3 were used in more than two sites/settings. RE3 was selected in all sites except ABNP.

NIR2 was used in both NPKA settings and SOFO but not in CBNP or ABNP. SWIR2 was included in all settings except NPKA_ALS and ABNP. Notably, the blue and green bands were not selected in any of the sites.

3.2. Results of the RF regression

Pixel-level age maps were generated for each of the four test sites. The results presented in this section refer to model performance validation based on the previously described 90/10 data splitting strategy. The RF model yielded the accuracy values reported in Table 4.

Similar to previous studies based on RF regression, the models tend to overestimate the age of young forests and underestimate age of old forests (Besnard et al., 2021). This effect is illustrated in the scatterplots for CBNP and NPKA_ALS (Fig. 5). Such over- and underestimation typically results in low bias values; therefore, RMSE is used as the primary metric for evaluating model performance. The inclusion of ALS data clearly improves model performance, with RMSE reductions of 9.2 years for NPKA and 4.6 years for SOFO (see Table 4). Notably, the error range for CBNP and ABNP without ALS is similar to SOFO and NPKA with ALS. In addition, we calculated R2 for the same 10 % subset used for RMSE (Table 4). While RMSE and R2 are widely reported indicators of model accuracy, they primarily reflect internal validation and may

Table 4
Accuracy assessment values based on the 90/10 split.

	SOFO	SOFO_ALS	NPKA	NPKA_ALS	CBNP	ABNP
RMSE [yrs]	52.5	47.9	50.0	40.8	41.3	41.2
R^2	0.352	0.526	0.484	0.625	0.62	0.617

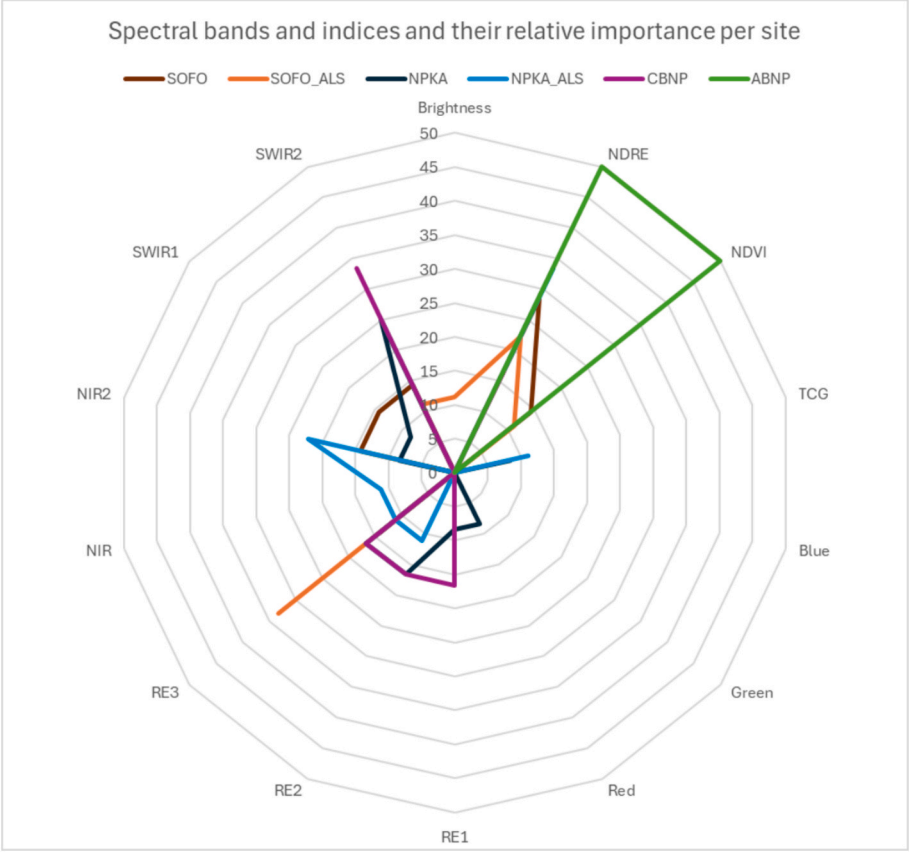

Fig. 4. Used spectral features (bands and indices) in the different sites depicted in percent of totally used features per site/setting (including ALS or not).

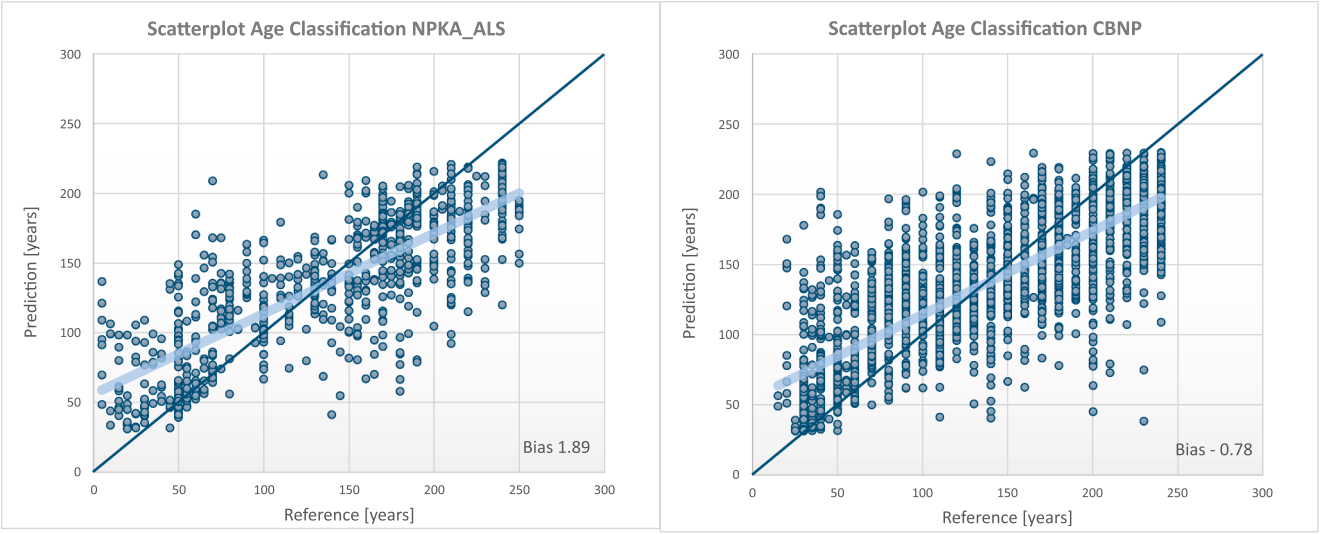

Fig. 5. Scatterplots of age prediction versus reference for CBNP (left) and NPKA_ALS (right).

not fully capture the model's ability to generalize to independent datasets. This aspect is addressed in Section 3.3, where the aggregated development classes determined by field assessments are analyzed.

3.3. Results compared to independent field data

The regression estimator results were used to classify each pixel into the same development classes identified during field inspections (see Table 3 for class definitions). The initial blind classification approach produced OA values ranging from 0.26 (ABNP) to 0.70 (SOFO with ALS data). However, these values do not account for spatial uncertainties such as minor geolocation errors or local structural heterogeneity within forest stands. To address these limitations, a plausibility-based shift analysis was conducted (see Section 2.3.4). The results of both the blind classification and the plausibility-based assessments are summarized in Table 5. Depending on site and input data, the plausibility analysis improved OA by 17 %–24 %. These findings suggest that a substantial portion of the apparent misclassifications in the blind approach were likely due to minor spatial misalignments rather than actual inaccuracies in the model. This highlights the relevance of incorporating spatial plausibility checks to achieve a more accurate and realistic evaluation of classification performance.

Overall, the classification performance can be considered sufficient for SOFO and NPKA, while the OA for ABNP (0.53) and CBNP (0.56) remains relatively low when using the five structural classes. However, when the five classes are aggregated into two broader categories, the classification accuracy improves significantly. The two classes are:

- Non-OGF (NOGF): Includes the initial phase (IP), stem exclusion phase (EP), advanced phase (AP), and mature phase (MP).
- OGF (class OP): Represents old-growth forests.

It is important to note that this aggregation reflects a typical operational and political scenario, aligning with the EU's requirements, rather than providing a complete structural typology. For the plausibility-based assessment, accuracy improved between 3 % (CBNP) and 11 % (ABNP) compared to the five-class approach. The highest accuracy levels were achieved for SOFO (94 %) and NPKA (88 %) when ALS data were included in the analysis. Detailed error matrices can be found in Appendix B.

3.4. Resulting maps

For all four sites, maps depicting forest age, structural development classes, and OGF/Non-OGF classifications were generated. To maintain brevity, only one example is presented below (Fig. 6). Maps for the other test sites are provided in the Discussion section, where they are compared to existing datasets.

4. Discussion and conclusions

Regarding feature importance, the results show that ground elevation was the only variable consistently ranked among the top eight across all study sites. This finding aligns with expectations, as protected areas are often located in regions with older forest stands, a pattern previously noted (Joppa and Pfaff, 2009; Sabatini et al., 2018). The importance of elevation was lowest in SOFO, which is consistent with its predominantly flat terrain (rank 8 and 6 resp.). In contrast, elevation played a significantly more prominent role in mountainous regions, ranking 6th for CBNP, 4th for ABNP, and 3rd in both NPKA settings. The central role of ground elevation has also been emphasized in prior studies (Dobrinić et al., 2021).

In contrast to comparable studies (Adiningrat et al., 2024), where the three most important features for age classification were ALS-derived

Table 5
Accuracy assessment values compared to independent field measurements in the blind/plausibility approach. Recall and Precision are macro-averaged (e.g. computed per class and averaged equally across all classes).

		SOFO	SOFO_ALS	NPKA	NPKA_ALS	ABNP	CBNP
OA	5 classes	0.60/0.81	0.70/0.87	0.53/0.72	0.55/0.78	0.26/0.53	0.31/0.56
	2 classes	0.66/0.88	0.78/0.94	0.61/0.80	0.69/0.88	0.37/0.64	0.34/0.59
Recall	5 classes	0.27/0.36	0.29/0.37	0.24/0.35	0.22/0.41	0.16/0.32	0.19/0.28
	2 classes	0.68/0.90	0.73/0.92	0.60/0.79	0.67/0.88	0.36/0.65	0.49/0.71
Precision	5 classes	0.24/0.32	0.30/0.36	0.20/0.28	0.19/0.49	0.10/0.21	0.19/0.25
	2 classes	0.66/0.86	0.80/0.95	0.61/0.81	0.67/0.87	0.36/0.64	0.49/0.65

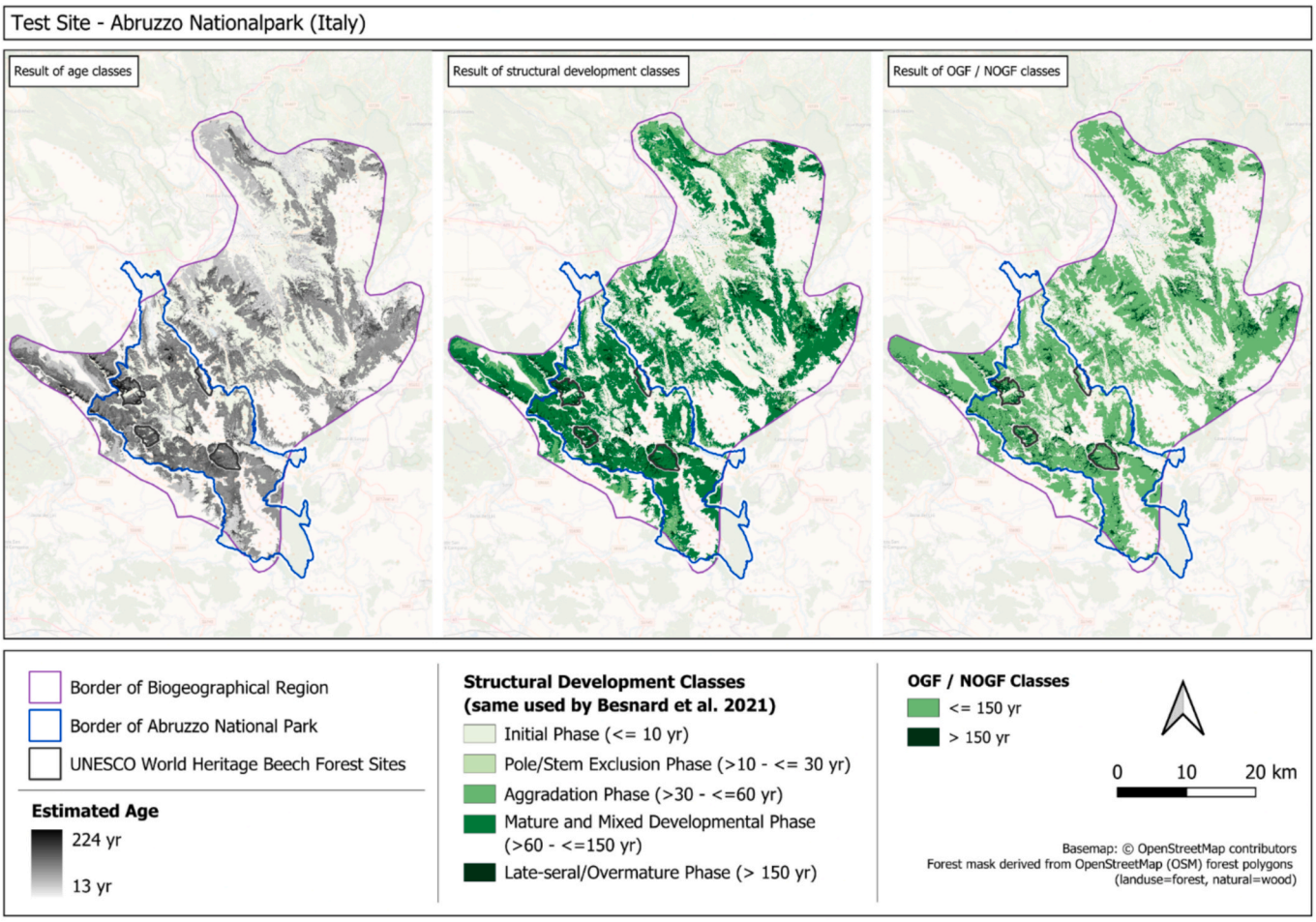

Fig. 6. Resulting maps from left to right: estimated age; structural development classes and potential OGF classification for ABNP.

structural metrics, only canopy cover in NPKA exceeded the 1 % feature importance threshold and was included in the age classification. A plausible explanation for this difference in performance may lie in the dominant tree species within the study areas. While the present study focuses on beech-dominated forests, the study area of Adiningrat et al. (2024) consists predominantly of Norway spruce (Picea abies). It is well established that tree species exhibit distinct canopy surface characteristics due to their specific crown shapes (Liu et al., 2023; Pretzsch and Schütze, 2005). Beech forests, for instance, are known to form "cathedral-like" stand structures (Ellenberg, 1996). Additionally, older beech forests tend to have more canopy gaps compared to younger stands (Rugani et al., 2013). Another study (Bayer and Pretzsch, 2017) demonstrated that pure and mixed stands of Norway spruce (Picea abies) and European beech (Fagus sylvatica) respond differently to gap cutting. Their findings suggest that spruce primarily allocates newly available above-ground resources to increasing diameter at breast height (DBH), whereas beech prioritizes rapid occupation of canopy space (Bayer and Pretzsch, 2017). As a result, the canopy surface shape in spruce-dominated forests is likely to exhibit greater age-related variability compared to beech-dominated forests. This explains why structural parameters, such as the rumple index or the standard deviation of vegetation height, are less effective for predicting age in beech-dominated forests.

The maximum vegetation height derived from ALS data was identified as the second most important feature in both study areas with ALS data available (NPKA_ALS and SOFO_ALS). In case of NPKA, additional features such as mean vegetation height (Mean_Veg_Height) and terrain slope also contributed to the age classification. It is well established that tree height and age are generally correlated, particularly during the early stages of growth. However, this relationship tends to plateau as trees reach a certain age, at which point height increment slows down and resources are increasingly allocated to diameter at breast height (DBH) growth instead (Oliver et al., 1996).

Regarding the feature importance of spectral bands, both similarities and differences compared to previous studies can be observed. Similar to a previous study (Adiningrat et al., 2024), the NIR band (in our case, the 20 m NIR band) was identified as an important feature. The red edge spectral bands also proved to be relevant; however, unlike previous studies (Adiningrat et al., 2024; Astola et al., 2019), which identified RE1 as the most important red edge band, our study found RE3 to be used more frequently. Consistent with existing literature, the SWIR bands were highly important, while the blue, green, and red bands were relatively less utilized (Adiningrat et al., 2024; Astola et al., 2019; Dobrinić et al., 2021). Interestingly, in contrast to these studies – which reported that commonly used vegetation indices (e.g., NDVI, EVI, or SAWI) provided limited information – we identified one vegetation index of notable importance: NDRE1. It is worth noting, however, that none of the aforementioned studies included NDRE1 in their analyses.

Our findings align with previous research, highlighting the significant benefits of using texture features for classification tasks. This has been demonstrated in studies on OGF classification (Adiningrat et al., 2024) and general land cover classification (Dobrinić et al., 2021), although the latter utilized GLCM derived from Sentinel-1 data. In our study, Sentinel-2 texture metrics ranked among the highest features for SOFO (occupying all top three ranks for SOFO without ALS and rank 3 for SOFO with ALS) and ABNP (ranks 3, 5, and 6). These results indicate

that the importance of texture features can vary significantly depending on the biogeographical and topographic context of the study area.

We compared our results to existing maps of primary forests in Europe (Sabatini et al., 2020) and global forest age classification (Besnard et al., 2021), as shown in Figs. 7–10. As expected, a global data set (Besnard et al., 2021) lacks the spatial resolution necessary for detailed assessments. While it does capture the spatial distribution of mature and young forests in some cases, such as ABNP (Fig. 7), the patterns in other areas, such as SOFO (Fig. 9) and NPKA (Fig. 10) differ significantly from our results. In addition, the global data set (Besnard et al., 2021) seem to underrepresent the oldest structural development class (OP). For instance, in ABNP, the dataset identifies only a limited number of pixels as OP, while in other sites, no OP areas are classified, despite the documented presence of old and primary forests in these regions (Sabatini et al., 2021,2020). These findings underscore the limitations of relying solely on global datasets for local planning and decision-making, as they might fail to accurately capture local conditions and forest characteristics.

Our results show strong alignment with the European primary forest database (Sabatini et al., 2020,2021), which is a collection of existing data from various sources, including in-situ assessments. The best spatial match was observed for CBNP (see Fig. 8), despite this site having the lowest accuracy values based on independent validation among the four study areas. One possible explanation for this good spatial fit is that our training data and the European primary forest database may have originated from the same local source, such as the national park administration. The CBNP example notably demonstrates the potential of remote sensing (RS)-based mapping to enhance targeted field surveys. By prioritizing areas classified as OP, such as the region highlighted in Fig. 8, field assessment resources can be allocated more efficiently to verify and designate old-growth forests (OGFs) for conservation purposes (Barredo et al., 2021; Sabatini et al., 2021).

In terms of classification accuracy, our results for OGF/non-OGF classification are comparable to those reported in the literature for the Bavarian Forest National Park, where an overall accuracy (OA) of 92 % was achieved integrating ALS data and 71 % using Sentinel-2 data alone (Adiningrat et al., 2024). Similar results were obtained for SOFO, located in the flat Atlantic biogeographical region, with an OA of 94 % including ALS data and 88 % without ALS. Likewise, in NPKA, situated in the Central Alps, we achieved an OA of 88 % with ALS and 80 % without ALS. It is important to note that the results reported for the Bavarian Forest (Adiningrat et al., 2024) were based on a training/test split of polygon-based maps, whereas our accuracy assessments are derived from independent field plot data, which typically leads to lower accuracy estimates.

Nonetheless, it is important to acknowledge that the results for the other two sites are significantly lower, with overall accuracies (OAs) of only 59 % for CBNP and 64 % for ABNP. One possible explanation for this discrepancy could be differences in local growing conditions, such as soil or climatic factors. However, these environmental variables should be adequately represented in the training data and are therefore unlikely to be the primary cause of the reduced performance. Instead, the quality of the training data and the degree of congruence between the training and validation datasets are likely more influential factors affecting model accuracy (Lauria and Tayi, 2008). In our study areas, the age maps used for training are not always spatially homogeneous and may be outdated in certain locations. This issue is exemplified in ABNP, where we analyzed a training polygon assigned an age of 100 years. This polygon was investigated in the field and covered by 19 validation plots. The comparison between field assessments and remote sensing

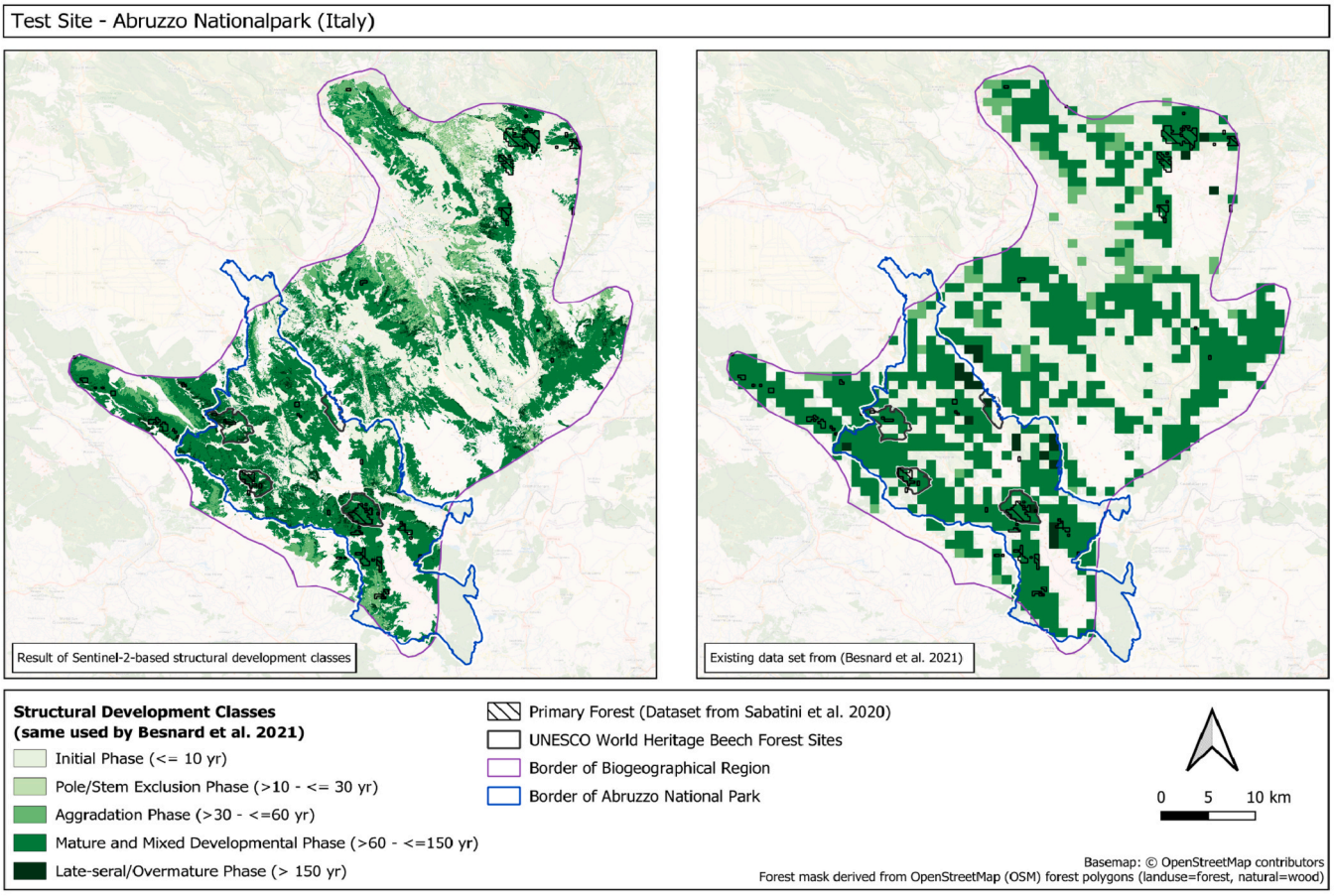

Fig. 7. Result for the five structural development classes in ABNP in comparison to existing data sets.

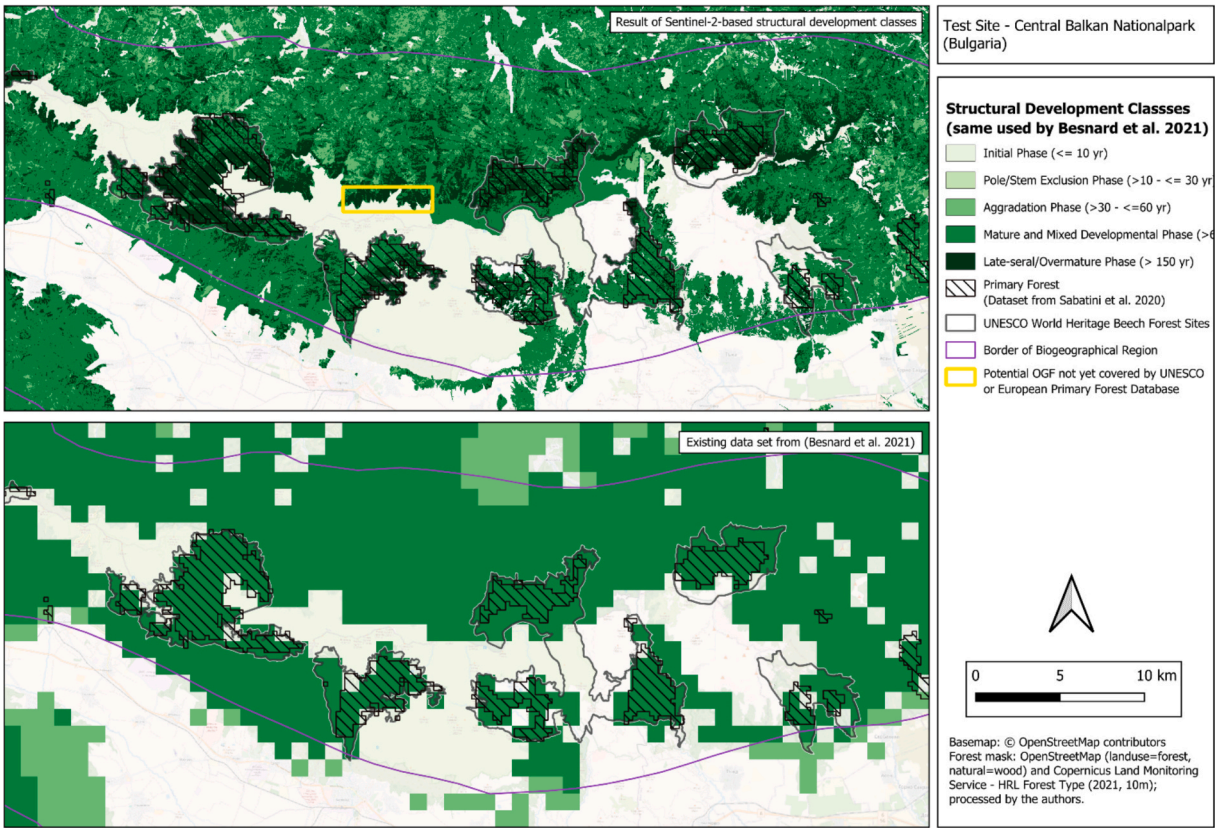

Fig. 8. Result for the five structural development classes in CBNP in comparison to existing data sets and highlighting an area of potential OGF not yet covered by UNESCO or the European Primary Forest Database.

classifications for this polygon is illustrated in Fig. 11. For this polygon, two plots were clearly located within small canopy gaps (field plot assigned to class IP), which were neither captured by remote sensing nor represented in the polygon map used for training. Additionally, one plot (5.26 %) was assigned to the AP class, while more than 60 % of the plots were assessed as MP, compared to 81 % MP based on the remote sensing results. The proportions of OP are very similar, with field assessments indicating 19 % OP compared to 21 % OP in the RS classification.

Another potential source of classification error arises from the discrepancy between age as a continuous value and the use of discrete development classes as reference data. For instance, if a pixel is assigned an estimated age of 59 years, it would be assigned to class AP. However, if the corresponding field assessment categorizes the same plot as belonging to the MP (starting at an age limit of 60 years), this would be counted as a misclassification in the accuracy assessment, despite the actual age difference being minimal. Such errors result from the rigid class boundaries applied in the classification scheme, which fail to account for gradual transitions between forest development stages. This is especially true, if reference age maps are given in rough categories only. This issue is particularly pronounced when reference age maps are provided in broad categories, as is the case for CBNP and illustrated in Fig. 5.

In summary, the findings of this study address the research questions and lead to the following conclusions: Remote sensing (RS)-based classification has proven to be broadly applicable across diverse regions in Europe for identifying areas of potential OGF. The accuracy of the classification appears to be influenced more by the quality of the training data than by the biogeographic region itself. The achievable OA for classifying structural development classes of beech forests from RS data, validated with independent field-measured plot data, varies considerably: from 53 % to 87 % for five classes and from 59 % to 94 % when the classes are aggregated into two broader categories. Lower accuracies were generally observed for Bulgarian and Italian sites compared to the Austrian and Belgium sites. The inclusion of ALS data improved overall classification accuracy by 6 %, with ALS-derived height metrics proving to be far more influential than structural features. Based on these results, it is strongly recommended to integrate ALS data into the classification process wherever available, as this significantly enhances the reliability of RS-based forest structural assessments.

This study focuses exclusively on beech and beech-dominated forests, and as such, the conclusions cannot be directly generalized to forests dominated by other tree species. Comparisons with similar studies on non-beech forests reveal slightly different results, highlighting the need for stratification based on dominant species (or species groups) to achieve robust classification outcomes. Even in this study, which relies on an extensive dataset of field observations and existing age maps, the quality of reference data remains a critical issue. Discrepancies between age maps and field plots were observed, and additional limitations related to plot size and geolocation accuracy were evident, particularly in forested mountain environments typical of OGFs. Furthermore, the availability, accessibility, and homogeneity of ALS data – especially in Eastern and Southern Europe – continue to be significant constraints for large-scale, European-wide applications. Although our structural development classification includes parameters like canopy gaps, deadwood and tree microhabitats indirectly, these features are not assessed individually. This limitation contributes to the conclusion that the accuracy of RS results is not sufficient to fully replace field assessments. This finding aligns with previous studies (Adiningrat et al., 2024; Garbarino et al., 2012; Hirschmugl et al., 2023b), particularly given the complexity and diversity of indicators that define OGFs, such as deadwood volume and the presence of specialized biota.

Building on the identified limitations, future research should focus on integrating joint assessments of OGF regarding various tree species

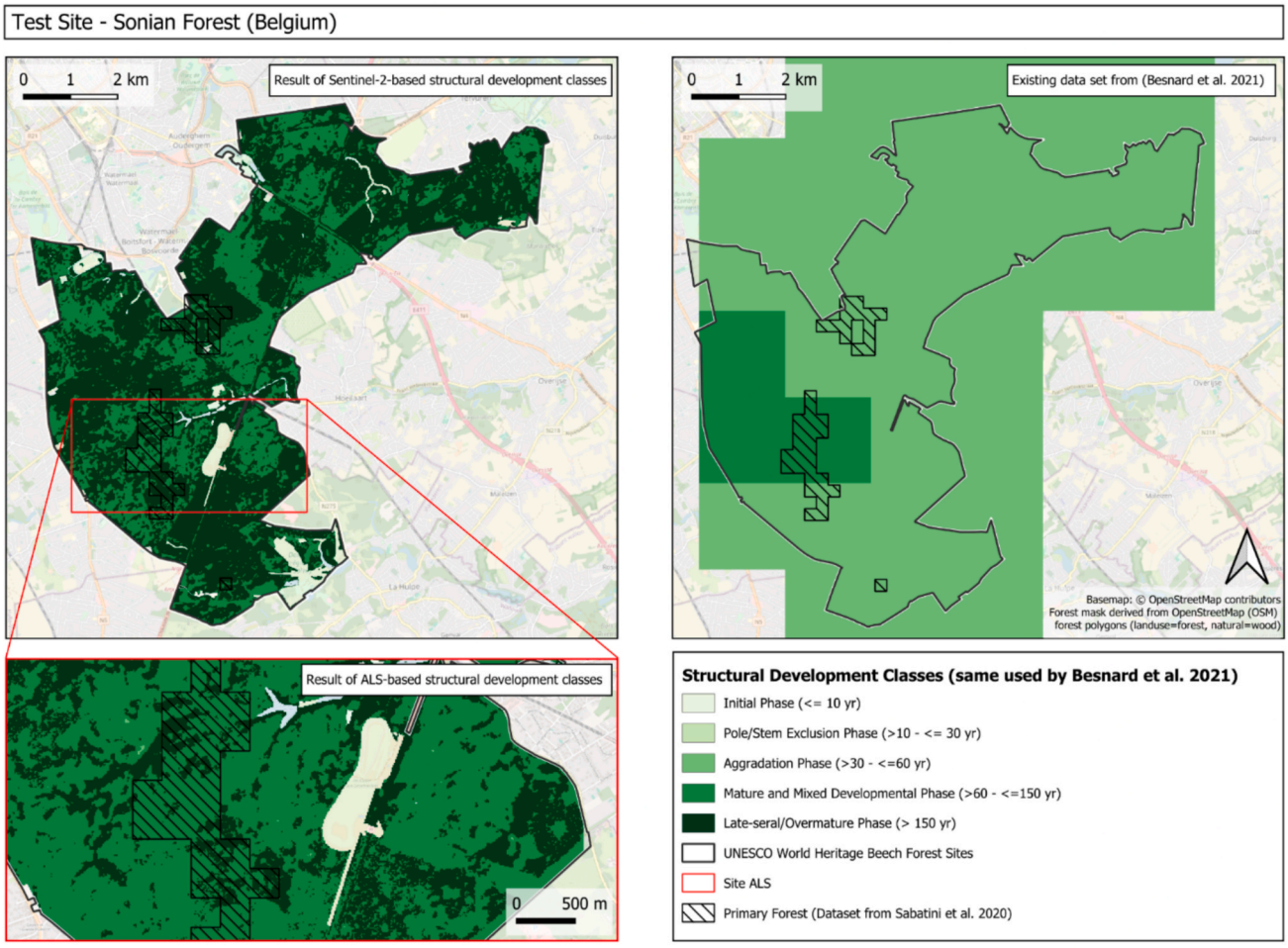

Fig. 9. Result for the five structural development classes in SOFO in comparison to existing data sets.

enabling a broader application of the RS-based mapping approach. Another promising research direction is to adopt a parameter-based approach, as previously outlined (Hirschmugl et al., 2023b), which is supported by advancements in the detection of deadwood (Jarron et al., 2021; Lin et al., 2024; Wing et al., 2015) and the classification of structural forest parameters (Fischer et al., 2024; Ross et al., 2024) using ALS data. However, for such approaches to be successful, open and FAIR (Findable, Accessible, Interoperable, and Reusable) data policies must be implemented and realized across Europe, both for ALS data and field-measured forest data.

Finally, our study has demonstrated that remote sensing can provide valuable spatial insights into potential OGF locations. When combined with protected area maps, RS offers an effective tool to better target field visits and facilitate the faster identification of currently unprotected OGFs. This is particularly critical in the eastern and southeastern regions of Europe, where alternative data sources are limited and the pressure on remaining OGFs is exceptionally high.

5. Declaration of generative AI and AI-assisted technologies in the manuscript preparation process

During the preparation of this work, the authors used Uni Graz's uniGPT tool, which is built on OpenAI's GPT-4 model for English language editing and polishing. After using this tool, the authors reviewed and edited the content as needed and take full responsibility for the content of the published article.

6. Data Source

UNESCO World Heritage (X): World Heritage Beech Forests. https://www.europeanbeechforests.org/ (16.07.24).

'Biogeographical regions, Europe 2016, ver. 1', 2016, accessed 2025-12-30, http://data.europa.eu/88u/dataset/c6d27566-e699-4d58-a132-bbe3fe01491b https://data.europa.eu/data/datasets/data_biogeographical-regions-europe-2005?locale.

7. Disclaimer/publisher's note

The statements, opinions and data contained in all publications are solely those of the individual author(s) and contributor(s) and not of MDPI and/or the editor(s). MDPI and/or the editor(s) disclaim responsibility for any injury to people or property resulting from any ideas, methods, instructions or products referred to in the content.

CRediT authorship contribution statement

Manuela Hirschmugl: Writing – review & editing, Writing – original draft, Project administration, Methodology, Data curation, Conceptualization. **Carina Sobe:** Visualization, Software, Formal analysis, Data curation. **Peter Meyer:** Writing – review & editing, Data curation. **Hanns Kirchmeir:** Data curation. **Alfredo Di Filippo:** Data curation. **Ruth Vanhaecht:** Project administration. **Yanitsa Ivanova:** Data curation. **Kris Vandekerkhove:** Writing – review & editing, Supervision, Funding acquisition, Data curation, Conceptualization.

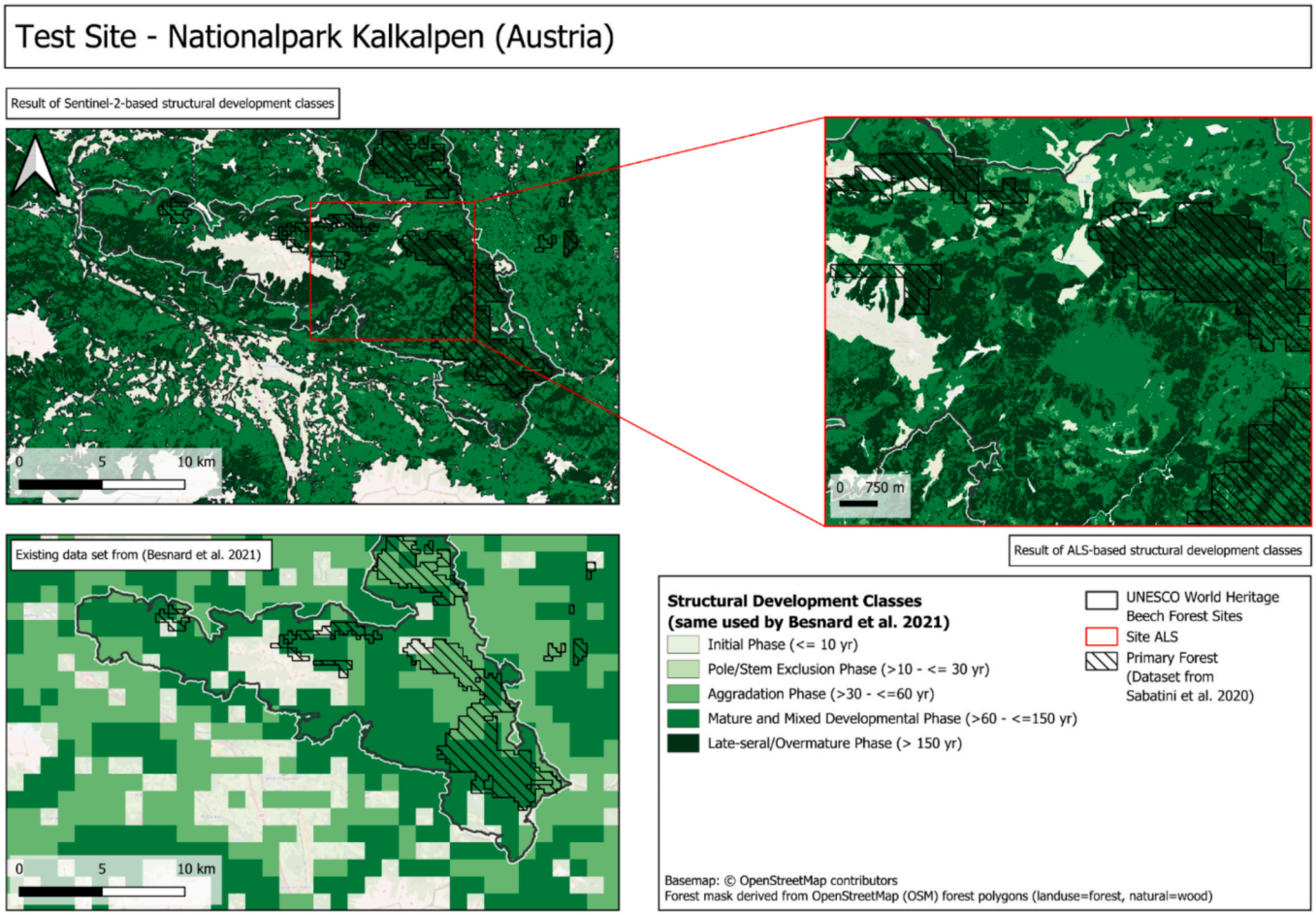

Fig. 10. Result for the five structural development classes in NPKA in comparison to existing data sets.

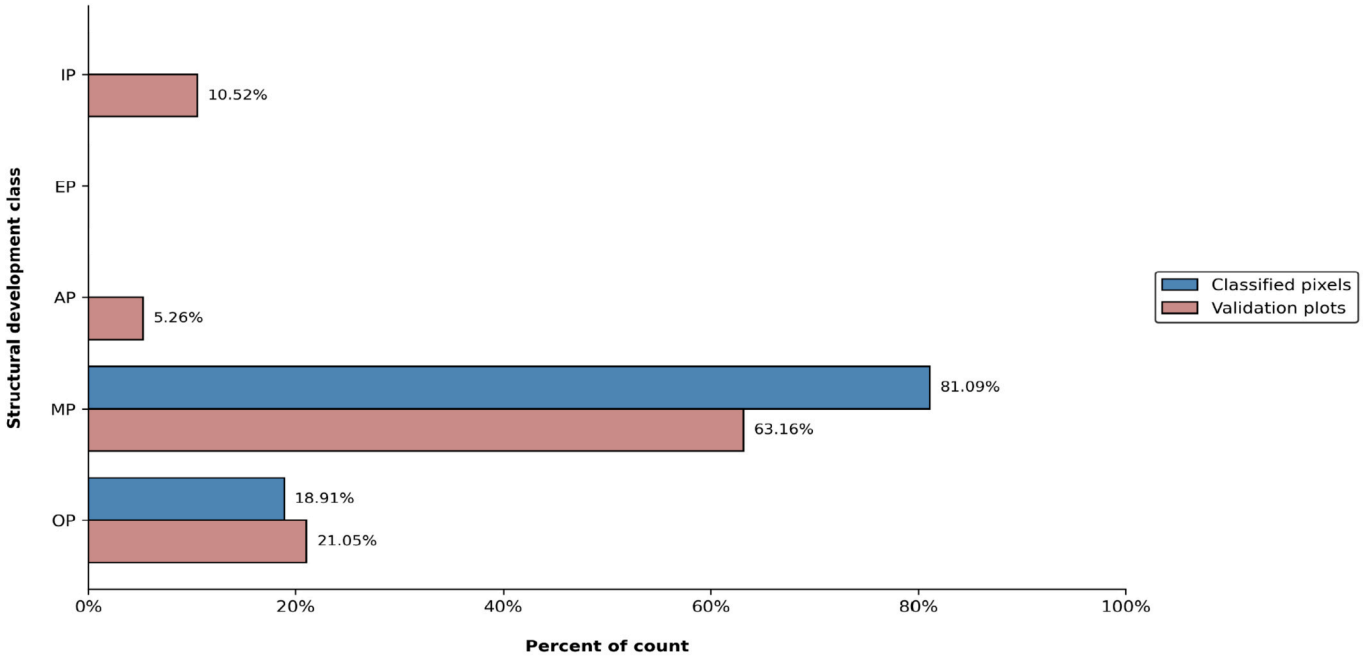

Fig. 11. Comparison of field plots and RS results for one training polygon (given age: 100 years) in ABNP.

Funding

This research was funded by the LIFE Programme of the European Commission under Grant Agreement "LIFE20 PRE/BE/0000111 – LIFE PROGNOSES".

Declaration of competing interest

The authors declare that they have no known competing financial interests or personal relationships that could have appeared to influence the work reported in this paper.

Acknowledgments

We would like to thank all partners of the LIFE + PROGNOSES project for their great cooperation and especially partners of the study sites for providing the age maps for training and the field work for validation, as well as for their feedback on previous versions of the classification. We further would like to thank the anonymous reviewers for their constructive feedback, that helped improving the earlier version of this manuscript.

Appendix A. List of abbreviations

Abbreviation	Description
ABNP	Abruzzo National Park
ALS	Airborne Laser Scanning
AP	Aggregation Phase
ASM	Angular Second Moment
B1-B12	Sentinel-2 spectral bands
BOA	Bottom of Atmosphere
CBD	Convention on Biological Diversity
CBNP	Central Balkan National Park
DEM	Digital Elevation Model
EP	Exclusion Phase
EU	European Union
GLCM	Gray-Level Co-occurrence Matrix
GNDVI	Green Normalized Difference Vegetation Index
IP	Initial Phase
LiDAR	Light Detection and Ranging
MP	Mature Phase
NDRE1	Normalized Difference Red Edge 1 Index
NDVI	Normalized Difference Vegetation Index
NPKA	Nationalpark Kalkalpen
OA	Overall Accuracy
OGF	Old-Growth Forest
OGI	Old-Growthiness Indicator
OP	Overmature Phase
Perc10	10th Percentile
Perc90	90th Percentile
RE1	Red Edge 1
RE2	Red Edge 1
RE3	Red Edge 1
RF	Random Forest
RGB	Red-Green-Blue Composite
RMSE	Root Mean Square Error
RS	Remote Sensing
SOFO	Sonian Forest
SRTM	Shuttle Radar Topography Mission
SWIR1	Short Wave-Infrared
SWIR2	Short Wave-Infrared
TCG	Tasseled Cap Greenness
TOA	Top of Atmosphere

Appendix B:. Error matrices

Error Matrix: ABNP (5 age classes and 2 age classes)

Classification

Reference	IP	EP	AP	MP	OP
ABNP_blind					
IP	0% (0)	0% (0)	0% (0)	100% (2)	0% (0)
EP	0% (0)	0% (0)	0% (0)	100% (1)	0% (0)
AP	0% (0)	0% (0)	0% (0)	32% (14)	68% (30)
MP	0% (0)	0% (0)	0% (0)	51% (19)	49% (18)
OP	0% (0)	0% (0)	0% (0)	70% (47)	30% (20)
ABNP_plausibility					
IP	0% (0)	0% (0)	0% (0)	100% (2)	0% (0)
EP	0% (0)	0% (0)	0% (0)	100% (1)	0% (0)
AP	0% (0)	0% (0)	0% (0)	32% (14)	68% (30)
MP	0% (0)	0% (0)	0% (0)	95% (35)	5% (2)
OP	0% (0)	0% (0)	0% (0)	33% (22)	67% (45)

Classification

Reference	NOGF	OGF
ABNP_blind		
NOGF	43% (36)	57% (48)
OGF	70% (47)	30% (20)
ABNP_plausibility		
NOGF	62% (52)	38% (32)
OGF	33% (22)	67% (45)

Values in () are absolute counts.

Error Matrix: CBNP (5 age classes and 2 age classes)

Classification

Reference	IP	EP	AP	MP	OP
NPKA_ALS_blind					
IP	0% (0)	0% (0)	0% (0)	100% (1)	0% (0)
EP	0% (0)	0% (0)	0% (0)	0% (0)	0% (0)
AP	0% (0)	0% (0)	0% (0)	86% (6)	14% (1)
MP	0% (0)	0% (0)	0% (0)	30% (3)	70% (7)
OP	0% (0)	0% (0)	0% (0)	23% (7)	77% (24)
NPKA_ALS_plausibility					
IP	0% (0)	0% (0)	0% (0)	100% (1)	0% (0)
EP	0% (0)	0% (0)	0% (0)	0% (0)	0% (0)
AP	0% (0)	0% (0)	29% (2)	57% (4)	14% (1)
MP	0% (0)	0% (0)	0% (0)	90% (9)	10% (1)
OP	0% (0)	0% (0)	0% (0)	13% (4)	87% (27)

Classification

Reference	NOGF	OGF
NPKA_ALS_blind		
NOGF	56% (10)	44% (8)
OGF	23% (7)	77% (24)
NPKA_ALS_plausibility		
NOGF	89% (16)	11% (2)
OGF	13% (4)	87% (27)

Values in () are absolute counts.

Error Matrix: NPKA_ALS (5 age classes and 2 age classes)
Error Matrix: NPKA_S2 (5 age classes and 2 age classes)
Error Matrix: SOFO_ALS (5 age classes and 2 age classes)

Classification

Reference	IP	EP	AP	MP	OP
SOFO_ALS_blind					
IP	0% (0)	0% (0)	0% (0)	0% (0)	0% (0)
EP	0% (0)	0% (0)	0% (0)	100% (4)	0% (0)
AP	0% (0)	0% (0)	0% (0)	100% (5)	0% (0)
MP	0% (0)	0% (0)	0% (0)	93% (62)	7% (5)
OP	0% (0)	0% (0)	0% (0)	48% (22)	52% (24)
SOFO_ALS_plausibility					
IP	0% (0)	0% (0)	0% (0)	0% (0)	0% (0)
EP	0% (0)	0% (0)	0% (0)	100% (4)	0% (0)
AP	0% (0)	0% (0)	0% (0)	100% (5)	0% (0)
MP	0% (0)	0% (0)	0% (0)	100% (67)	0% (0)
OP	0% (0)	0% (0)	0% (0)	15% (7)	85% (39)

Classification

Reference	NOGF	OGF
SOFO_ALS_blind		
NOGF	93% (71)	7% (5)
OGF	48% (22)	52% (24)
SOFO_ALS_plausibility		
NOGF	100% (76)	0% (0)
OGF	15% (7)	85% (39)

Values in () are absolute counts.

Error Matrix: SOFO_S2 (5 age classes and 2 age classes)

Classification

Reference	IP	EP	AP	MP	OP
SOFO_S2_blind					
IP	0% (0)	0% (0)	0% (0)	0% (0)	0% (0)
EP	0% (0)	0% (0)	0% (0)	100% (4)	0% (0)
AP	0% (0)	0% (0)	0% (0)	100% (5)	0% (0)
MP	0% (0)	0% (0)	0% (0)	59% (53)	41% (37)
OP	0% (0)	0% (0)	0% (0)	26% (12)	74% (34)
SOFO_S2_plausibility					
IP	0% (0)	0% (0)	0% (0)	0% (0)	0% (0)
EP	0% (0)	0% (0)	0% (0)	100% (4)	0% (0)
AP	0% (0)	0% (0)	0% (0)	100% (5)	0% (0)
MP	0% (0)	0% (0)	0% (0)	82% (74)	18% (16)
OP	0% (0)	0% (0)	0% (0)	4% (2)	96% (44)

Classification

Reference	NOGF	OGF
SOFO_S2_blind		
NOGF	63% (62)	37% (37)
OGF	26% (12)	74% (34)
SOFO_S2_plausibility		
NOGF	84% (83)	16% (16)
OGF	4% (2)	96% (44)

Values in () are absolute counts.

All appendix sections must be cited in the main text. In the appendices, Figures, Tables, etc. should be labeled starting with "A"—e.g., Fig. A1, Fig. A2, etc.

Data availability

Our data is uploaded on Zenodo: field plot data is available at https://zenodo.org/records/14718750 and the resulting RS maps are available at (https://zenodo.org/records/17276266). The biogeographical regions of Europe are available at https://data.europa.eu/data/datasets/c6d27566-e699-4d58-a132-bbe3fe01491b?locale=de. The outlines of the Unesco World Heritage Beech Forest sites are available upon request from the individual site managing entities to be found at https://www.europeanbeechforests.org/world-heritage-beech-forests.

References

Adiningrat, D. P., Schlund, M., Skidmore, A. K., Abdullah, H., Wang, T., & Heurich, M. (2024). Mapping temperate old-growth forests in Central Europe using ALS and Sentinel-2A multispectral data. *Environmental Monitoring and Assessment, 196*, 841. https://doi.org/10.1007/s10661-024-12993-5

Astola, H., Häme, T., Sirro, L., Molinier, M., & Kilpi, J. (2019). Comparison of Sentinel-2 and Landsat 8 imagery for forest variable prediction in boreal region. *Remote Sensing of Environment, 223*, 257–273. https://doi.org/10.1016/j.rse.2019.01.019

Barredo, J.I., Brailescu, C., Teller, A., Sabatini, F.M., Mauri, A., Janouskova, K., European Commission, Joint Research Centre (2021). Mapping and assessment of primary and old-growth forests in Europe.

Bauhus, J., Puettmann, K., & Messier, C. (2009). Silviculture for old-growth attributes. *Forest Ecology and Management, 258*, 525–537. https://doi.org/10.1016/j.foreco.2009.01.053

Bayer, D., & Pretzsch, H. (2017). Reactions to gap emergence: Norway spruce increases growth while European beech features horizontal space occupation – evidence by repeated 3D TLS measurements. *Silva Fennica, 51*, 10.14214/sf.7748.

Belgiu, M., & Drăguţ, L. (2016). Random forest in remote sensing: A review of applications and future directions. *ISPRS Journal of Photogrammetry and Remote Sensing, 114*, 24–31.

Besnard, S., Koirala, S., Santoro, M., Weber, U., Nelson, J., Gütter, J., Herault, B., Kassi, J., N'Guessan, A., Neigh, C., Poulter, B., Zhang, T., & Carvalhais, N. (2021). Mapping global forest age from forest inventories, biomass and climate data. *Earth System Science Data, 13*, 4881–4896. https://doi.org/10.5194/essd-13-4881-2021

Boiarskii, B. (2019). Comparison of NDVI and NDRE indices to detect differences in vegetation and chlorophyll content. *Journal of Mechanics of Continua and Mathematical Scientist, spl1*, Article 10.26782/jmcms.spl.4/2019.11.00003.

Breiman, L. (2001). Random forests. *Machine Learning, 45*, 5–32.

Brockerhoff, E. G., Barbaro, L., Castagneyrol, B., Forrester, D. I., Gardiner, B., González-Olabarria, J. R., Lyver, P. O., Meurisse, N., Oxbrough, A., Taki, H., Thompson, I. D., Van Der Plas, F., & Jactel, H. (2017). Forest biodiversity, ecosystem functioning and the provision of ecosystem services. *Biodiversity and Conservation, 26*, 3005–3035. https://doi.org/10.1007/s10531-017-1453-2

Buchwald, E. (2005). A hierarchical terminology for more or less natural forests in relation to sustainable management and biodiversity conservation. Presented at the Third Expert Meeting on Harmonizing Forest-related Definitions, Food and Agriculture Organization of the United Nations, Rome.

Burrascano, S., Keeton, W. S., Sabatini, F. M., & Blasi, C. (2013). Commonality and variability in the structural attributes of moist temperate old-growth forests: A global review. *Forest Ecology and Management, 291*, 458–479. https://doi.org/10.1016/j.foreco.2012.11.020

Carlson, T. N., & Ripley, D. A. (1997). On the relation between NDVI, fractional vegetation cover, and leaf area index. *Remote Sensing of Environment, 62*, 241–252. https://doi.org/10.1016/S0034-4257(97)00104-1

Christensen, M., Hahn, K., Mountford, E. P., Ódor, P., Standovár, T., Rozenbergar, D., Diaci, J., Wijdeven, S., Meyer, P., Winter, S., & Vrska, T. (2005). Dead wood in European beech (Fagus sylvatica) forest reserves. *Forest Ecology and Management, 210*, 267–282. https://doi.org/10.1016/j.foreco.2005.02.032

Ciocîrlan, M. I. C., Curtu, A. L., & Radu, G. R. (2022). Predicting leaf phenology in forest tree species using UAVs and satellite images: a case study for European beech (Fagus sylvatica L.). *Remote Sensing, 14*, 6198. https://doi.org/10.3390/rs14246198

Cohen, W. B., Spies, T. A., & Fiorella, M. (1995). Estimating the age and structure of forests in a multi-ownership landscape of western Oregon, U.S.A. *International Journal of Remote Sensing, 16*, 721–746. https://doi.org/10.1080/01431169508954436

Curovic, M., Spalevic, V., Sestras, P., Motta, R., Catalina, D. A. N., Garbarino, M., Vitali, A., & Urbinati, C. (2020). Structural and ecological characteristics of mixed broadleaved old-growth forest (Biogradska Gora-Montenegro). *Turkish Journal of Agriculture and Forestry, 44*, 428–438.

Czerwinski, C. J., King, D. J., & Mitchell, S. W. (2014). Mapping forest growth and decline in a temperate mixed forest using temporal trend analysis of Landsat imagery, 1987–2010. *Remote Sensing of Environment, 141*, 188–200. https://doi.org/10.1016/j.rse.2013.11.006

da Silva, L. P., Heleno, R. H., Costa, J. M., Valente, M., Mata, V. A., Gonçalves, S. C., da Silva, A. A., Alves, J., & Ramos, J. A. (2019). Natural woodlands hold more diverse, abundant, and unique biota than novel anthropogenic forests: A multi-group assessment. *European Journal of Forest Research, 138*, 461–472. https://doi.org/10.1007/s10342-019-01183-5

Digitaal Vlaanderen (2023). HANDLEIDING EODaS – Open LiDAR portaal (Rapport No. Versie 3). Digitaal Vlaanderen, EODaS + VITO, Brussels. https://remotesensing.vlaanderen.be/apps/openlidar/EODaS_openlidar_Handleiding.pdf.

Dobrinić, D., Gašparović, M., & Medak, D. (2021). Sentinel-1 and 2 time-series for vegetation mapping using random forest classification: A case study of Northern Croatia. *Remote Sensing, 13*, 2321. https://doi.org/10.3390/rs13122321

Drusch, M., Bello, U. D., Carlier, S., Colin, O., Fernandez, V., Gascon, F., Hoersch, B., Isola, C., Laberinti, P., Martimort, P., Meygret, A., Spoto, F., Sy, O., Marchese, F., & Bargellini, P. (2012). Sentinel-2: ESA's optical high-resolution mission for GMES operational services. *Remote Sensing of Environment, 120*, 25–36. https://doi.org/10.1016/j.rse.2011.11.026

Duncker, P. S., Barreiro, S. M., Hengeveld, G. M., Lind, T., Mason, W. L., Ambrozy, S., & Spiecker, H. (2012). Classification of forest management approaches: A new conceptual framework and its applicability to european forestry. *Ecology and Society, 17*, art51. https://doi.org/10.5751/ES-05262-170451

Ellenberg, H. (1996). *Vegetation Mitteleuropas mit den Alpen: In ökologischer, dynamischer und historischer Sicht*. Stuttgart: Ulmer.

ESA (2023). S2 MPC: Multi-layer Copernicus sentinel-2 GRI in level-1C – Product handbook.

Espinoza, C. Z., Khot, L. R., Sankaran, S., & Jacoby, P. W. (2017). High resolution multispectral and thermal remote sensing-based water stress assessment in subsurface irrigated grapevines. *Remote Sensing, 9*, 961. https://doi.org/10.3390/rs9090961

European Commission (2024). Regulation (EU) 2024/1991 of the European Parliament and of the Council of 24 June 2024 on nature restoration and amending Regulation (EU) 2022/869 (Text with EEA relevance), ISSN 1977-0677.

European Commission, 2023. Commission Guidelines for Defining, Mapping, Monitoring and Strictly Protecting EU Primary and Old-Growth Forests (Commission Staff Working Document No. 62). Brussels.

European Commission, 2020. COMMUNICATION FROM THE COMMISSION TO THE EUROPEAN PARLIAMENT, THE COUNCIL, THE EUROPEAN ECONOMIC AND SOCIAL COMMITTEE AND THE COMMITTEE OF THE REGIONS EU Biodiversity Strategy for 2030 Bringing nature back into our lives, COM/2020/380 final.

European Space Agency, 2015. Sentinel-2 User Handbook (Handbook), ESA Standard Document.

Farr, T. G., Rosen, P. A., Caro, E., Crippen, R., Duren, R., Hensley, S., Kobrick, M., Paller, M., Rodriguez, E., Roth, L., Seal, D., Shaffer, S., Shimada, J., Umland, J., Werner, M., Oskin, M., Burbank, D., & Alsdorf, D. (2007). The shuttle radar topography mission. *Reviews of Geophysics, 45*, Article 2005RG000183. https://doi.org/10.1029/2005RG000183

Feng, T., Chen, S., Feng, Z., Shen, C., & Tian, Y. (2021). Effects of canopy and multi-epoch observations on single-point positioning errors of a GNSS in coniferous and broadleaved forests. *Remote Sens., 13*, 2325. https://doi.org/10.3390/rs13122325

Fischer, F. J., Jackson, T., Vincent, G., & Jucker, T. (2024). Robust characterisation of forest structure from airborne laser scanning—A systematic assessment and sample workflow for ecologists. *Methods in Ecology and Evolution, 15*, 1873–1888. https://doi.org/10.1111/2041-210X.14416

Garbarino, M., Mondino, E. B., Lingua, E., Nagel, T. A., Dukić, V., Govedar, Z., & Motta, R. (2012). Gap disturbances and regeneration patterns in a Bosnian old-growth forest: A multispectral remote sensing and ground-based approach. *Annals of Forest Science, 69*, 617–625. https://doi.org/10.1007/s13595-011-0177-9

GILG, O., 2005. Old-growth forests: characteristics, conservation and monitoring. ISBN 2-912801-67-2.

Grabska-Szwagrzyk, E., Jakiel, M., Keeton, W., Kozak, J., Kuemmerle, T., Onoszko, K., Ostafin, K., Shahbandeh, M., Szubert, P., Szwagierczak, A., Szwagrzyk, J., Ziółkowska, E., & Kaim, D. (2024). Historical maps improve the identification of forests with potentially high conservation value. *Conservation Letters, 17*, Article e13043. https://doi.org/10.1111/conl.13043

Griffith, K. T., Ponette-González, A. G., Curran, L. M., & Weathers, K. C. (2015). Assessing the influence of topography and canopy structure on Douglas fir throughfall with LiDAR and empirical data in the Santa Cruz mountains, USA. *Environmenta Monitoring and Assessment, 187*. https://doi.org/10.1007/s10661-015-4486-6

Haralick, R. M., Shanmugam, K., & Dinstein, I. (1973). Textural features for image classification. *IEEE Transactions on Systems, Man, and Cybernetics, 3*, 610–621.

Healey, S., Cohen, W., Zhiqiang, Y., & Krankina, O. (2005). Comparison of Tasseled Cap-based Landsat data structures for use in forest disturbance detection. *Remote Sensing of Environment, 97*, 301–310. https://doi.org/10.1016/j.rse.2005.05.009

Hirschmugl, M., Lippl, F., & Sobe, C. (2023). Assessing the vertical structure of forests using airborne and spaceborne LiDAR data in the Austrian alps. *Remote Sensing, 15*, 664. https://doi.org/10.3390/rs15030664

Hirschmugl, M., Sobe, C., Di Filippo, A., Berger, V., Kirchmeir, H., & Vandekerkhove, K. (2023). Review on the possibilities of mapping old-growth temperate forests by remote sensing in Europe. *Environmental Modeling and Assessment, 28*, 761–785. https://doi.org/10.1007/s10666-023-09897-y

Jarron, L. R., Coops, N. C., MacKenzie, W. H., & Dykstra, P. (2021). Detection and Quantification of Coarse Woody Debris in Natural Forest Stands using Airborne LiDAR. *Forest Science, 67*, 550–563. https://doi.org/10.1093/forsci/fxab023

Jin, S., & Sader, S. A. (2005). Comparison of time series tasseled cap wetness and the normalized difference moisture index in detecting forest disturbances. *Remote Sensing of Environment, 94*, 364–372. https://doi.org/10.1016/j.rse.2004.10.012

Joppa, L. N., & Pfaff, A. (2009). High and far: Biases in the location of protected areas. *PLoS One1, 4*, e8273.

Kirchmeir, H., & Kovarovic, A. (2016). Nomination Dossier to the UNESCO for the Inscription on the World Heritage List „Primeval Beech Forests of the Carpathians and Other Regions of Europe" as extension to the existing Natural World Heritage Site „Primeval Beech Forests of the Carpathians and the Ancient Beech Forests of Germany" (1133bis). Klagenfurt.

Kirchmeir, H., Vandekerkhove, K., Di Filippo, A., Priori, S., Di Fiore, L., & Vanhaecht, R. (2023). Mapping guideline and field survey protocol for the Assessment of Old-Growth status and Ecosystem Services (Biodiversity & Carbon) in Beech Forests (Project Deliverable No. ACTION A.1.21 Field Mapping and Testing of Indicators).

Lauria, E. J. M., & Tayi, G. K. (2008). Statistical machine learning for network intrusion detection: A data quality perspective. *International Journal of Services Sciences, 1*, 179. https://doi.org/10.1504/ijssci.2008.019611

Laurin, G. V., Pirotti, F., Callegari, M., Chen, Q., Cuozzo, G., Lingua, E., Notarnicola, C., & Papale, D. (2017). Potential of ALOS2 and NDVI to estimate forest above-ground biomass, and comparison with Lidar-derived estimates. *Remote Sens., 9*, 18. https://doi.org/10.3390/rs9010018

Leibundgut, H., 1982. Europäische Urwälder der Bergstufe: dargestellt für Forstleute, Naturwissenschafter und Freunde des Waldes. P. Haupt, Bern.

Lin, D., Giannico, V., Lafortezza, R., Sanesi, G., & Elia, M. (2024). Use of airborne LiDAR to predict fine dead fuel load in Mediterranean forest stands of Southern Europe. *Fire Ecology, 20*, 58. https://doi.org/10.1186/s42408-024-00287-7

Liu, Y., You, H., Tang, X., You, Q., Huang, Y., & Chen, J. (2023). Study on individual tree segmentation of different tree species using different segmentation algorithms based on 3D UAV data. *Forests, 14*, 1327. https://doi.org/10.3390/f14071327

Luyssaert, S., Schulze, E.-D., Börner, A., Knohl, A., Hessenmöller, D., Law, B. E., Ciais, P., & Grace, J. (2008). Old-growth forests as global carbon sinks. *Nature, 455*, 213–215. https://doi.org/10.1038/nature07276

MacArthur, R. H., & MacArthur, J. W. (1961). On bird species diversity. *Ecology, 42*, 594–598. https://doi.org/10.2307/1932254

Martin, M., Cerrejón, C., & Valeria, O. (2021). Complementary airborne LiDAR and satellite indices are reliable predictors of disturbance-induced structural diversity in mixed old-growth forest landscapes. *Remote Sensing of Environment, 267*, Article 112746. https://doi.org/10.1016/j.rse.2021.112746

Mayrhofer, S., Kirchmeir, H., Weigand, E., & Mayrhofer, E. (2015). Assessment of forest wilderness in Kalkalpen National Park. *Ecomont J. Prot. Mt. Areas Res., 7*, 30–40. https://doi.org/10.1553/eco.mont-7-2s30

McRoberts, R. E. (2010). The effects of rectification and Global Positioning System errors on satellite image-based estimates of forest area. *Remote Sensing of Environment, 114*, 1710–1717. https://doi.org/10.1016/j.rse.2010.03.001

Menze, B. H., Kelm, B. M., Masuch, R., Himmelreich, U., Bachert, P., Petrich, W., & Hamprecht, F. A. (2009). A comparison of random forest and its Gini importance with standard chemometric methods for the feature selection and classification of spectral data. *BMC Bioinformatics, 10*, 213. https://doi.org/10.1186/1471-2105-10-213

Meyer, P., Aljes, M., Culmsee, H., Feldmann, E., Glatthorn, J., Leuschner, C., & Schneider, H. (2021). Quantifying old-growthness of lowland European beech forests by a multivariate indicator for forest structure. *Ecological Indicators, 125*, Article 107575. https://doi.org/10.1016/j.ecolind.2021.107575

Mikoláš, M., Piovesan, G., Ahlström, A., Donato, D. C., Gloor, R., Hofmeister, J., Keeton, W. S., Muys, B., Sabatini, F. M., Svoboda, M., & Kuemmerle, T. (2023). Protect old-growth forests in Europe now. *Science, 380*, 466. https://doi.org/10.1126/science.adh2303

Mikoláš, M., Ujházy, K., Jasík, M., Wiezik, M., Gallay, I., Polák, P., Vysoký, J., Čiliak, M., Meigs, G. W., & Svoboda, M. (2019). Primary forest distribution and representation in a central European landscape: Results of a large-scale field-based census. *Forest Ecology and Management, 449*, Article 117466.

Monnet, J.-M., Mermin, E., Chanussot, J., & Berger, F. (2010). Tree top detection using local maxima filtering: a parameter sensitivity analysis. Presented at the 10th international conference on lidar applications for assessing forest ecosystems (Silvilaser 2010), Freiburg, Germany (p. 9).

Motta, R., Garbarino, M., Berretti, R., Meloni, F., Nosenzo, A., & Vacchiano, G. (2015). Development of old-growth characteristics in uneven-aged forests of the Italian Alps. *European Journal of Forest Research, 134*, 19–31. https://doi.org/10.1007/s10342-014-0830-6

Munteanu, C., Senf, C., Nita, M. D., Sabatini, F. M., Oeser, J., Seidl, R., & Kuemmerle, T. (2021). Leveraging historical spy satellite photographs and recent remote sensing data to identify high conservation value forests. *Conservation Biology*. , Article cobi.13820. https://doi.org/10.1111/cobi.13820

Nikolov, I. D., & Dimitrov, M. A. (2023). Forest habitats on the territory of the National Park "Central Balkan" Bulgaria. *Hacquetia, 22*, 215–245. https://doi.org/10.2478/hacq-2022-0021

Nilsson, S. G., Niklasson, M., Hedin, J., Aronsson, G., Gutowski, J. M., Linder, P., Ljungberg, H., Mikusiński, G., & Ranius, T. (2003). Erratum to "Densities of large living and dead trees in old-growth temperate and boreal forests". *Forest Ecology and Management, 178*, 355–370. https://doi.org/10.1016/S0378-1127(03)00084-7

Oliver, C. D., Larson, B. C., & Oliver, C. D. (1996). *Forest stand dynamics* (update ed.). New York: Wiley.

Paillet, Y., Bergès, L., Hjältén, J., Ódor, P., Avon, C., Bernhardt-Römermann, M., Bijlsma, R., De Bruyn, L., Fuhr, M., Grandin, U., Kanka, R., Lundin, L., Luque, S., Magura, T., Matesanz, S., Mészáros, I., Sebastià-Teresa, M., Schmidt, W., Standovár, T., Tóthmérész, B., Uotila, A., Valladares, F., Vellak, K., & Virtanen, R. (2010). Biodiversity differences between managed and unmanaged forests: Meta-analysis of species richness in Europe. *Conservation Biology, 24*, 101–112. https://doi.org/10.1111/j.1523-1739.2009.01399.x

Piovesan, G., Bernabei, M., Di Filippo, A., Romagnoli, M., & Schirone, B. (2003). A long-term tree ring beech chronology from a high-elevation old-growth forest of Central Italy. *Dendrochronologia, 21*, 13–22. https://doi.org/10.1078/1125-7865-00036

Prasetiyowati, M. I., Maulidevi, N. U., & Surendro, K. (2021). Determining threshold value on information gain feature selection to increase speed and prediction accuracy of random forest. *Journal of Big Data, 8*. https://doi.org/10.1186/s40537-021-00472-4

Pretzsch, H., & Schütze, G. (2005). Crown allometry and growing space efficiency of norway spruce (Picea abies [L.] Karst.) and European beech (Fagus sylvatica L.) in pure and mixed stands. *Plant Biology, 7*, 628–639. https://doi.org/10.1055/s-2005-865965

Rengasamy, D., Mase, J. M., Kumar, A., Rothwell, B., Torres, M. T., Alexander, M. R., Winkler, D. A., & Figueredo, G. P. (2022). Feature importance in machine learning models: A fuzzy information fusion approach. *Neurocomputing, 511*, 163–174. https://doi.org/10.1016/j.neucom.2022.09.053

Roekaerts, M. (2002). The biogeographical regions map of Europe. basic principles of its creation and overview of its development. *(European Topic Centre Nature Protection and Biodiversity)*.

Ross, C. W., Loudermilk, E. L., O'Brien, J. J., & Snitker, G. (2024). Lidar-derived structural-complexity data across four experimental forests. *Data in Brief, 57*, Article 110955. https://doi.org/10.1016/j.dib.2024.110955

Rouse, J.W., Haas, R. H., Schell, J.A., & Deering, D.W. (1974). Monitoring vegetation systems in the Great Plains with ERTS. In: NASA. Goddard space flight center 3d ERTS-1 symp, sect a presented at the third earth resources technology satellite-1 symposium (Vol. 1, pp. 309–317).

Rugani, T., Diaci, J., & Hladnik, D. (2013). Gap dynamics and structure of two old-growth beech forest remnants in Slovenia. *PLoS One1, 8*, Article e52641. https://doi.org/10.1371/journal.pone.0052641

Sabatini, F. M., Bluhm, H., Kun, Z., Aksenov, D., Atauri, J. A., Buchwald, E., Burrascano, S., Cateau, E., Diku, A., Duarte, I. M., Fernández López, Á. B., Garbarino, M., Grigoriadis, N., Horváth, F., Keren, S., Kitenberga, M., Kiš, A., Kraut, A., Ibisch, P. L., Larrieu, L., Lombardi, F., Matovic, B., Melu, R. N., Meyer, P., Midteng, R., Mikac, S., Mikoláš, M., Mozgeris, G., Panayotov, M., Pisek, R., Nunes, L., Ruete, A., Schickhofer, M., Simovski, B., Stillhard, J., Stojanovic, D., Szwagrzyk, J., Tikkanen, O.-P., Toromani, E., Volosyanchuk, R., Vrška, T., Waldherr, M., Yermokhin, M., Zlatanov, T., Zagidullina, A., & Kuemmerle, T. (2021). European primary forest database v2.0. *Scientific Data, 8*, 220. https://doi.org/10.1038/s41597-021-00988-7

Sabatini, F. M., Burrascano, S., Keeton, W. S., Levers, C., Lindner, M., Pötzschner, F., Verkerk, P. J., Bauhus, J., Buchwald, E., Chaskovsky, O., Debaive, N., Horváth, F., Garbarino, M., Grigoriadis, N., Lombardi, F., Duarte, I. M., Meyer, P., Midteng, R., Mikac, S., Mikoláš, M., Motta, R., Mozgeris, G., Nunes, L., Panayotov, M., Ódor, P., Ruete, A., Simovski, B., Stillhard, J., Svoboda, M., Szwagrzyk, J., Tikkanen, O.-P., Volosyanchuk, R., Vrska, T., Zlatanov, T., & Kuemmerle, T. (2018). Where are Europe's last primary forests? *Diversity and Distributions, 24*, 1426–1439. https://doi.org/10.1111/ddi.12778

Sabatini, F. M., Keeton, W. S., Lindner, M., Svoboda, M., Verkerk, P. J., Bauhus, J., Bruelheide, H., Burrascano, S., Debaive, N., Duarte, I., Garbarino, M., Grigoriadis, N., Lombardi, F., Mikoláš, M., Meyer, P., Motta, R., Mozgeris, G., Nunes, L., Ódor, P., Panayotov, M., Ruete, A., Simovski, B., Stillhard, J., Svensson, J., Szwagrzyk, J., Tikkanen, O., Vandekerkhove, K., Volosyanchuk, R., Vrska, T., Zlatanov, T., & Kuemmerle, T. (2020). Protection gaps and restoration opportunities for primary forests in Europe. *Diversity and Distributions, 26*, 1646–1662. https://doi.org/10.1111/ddi.13158

Scientific Advisory Board on Forest Policy (2023). Managing old, close to nature deciduous forests in Germany in the context of biodiversity conservation, climate protection and adaptation to climate change. Berlin.

Sobe, C., Hirschmugl, M., & Wimmer, A. (2021). Sentinel-2 time series analysis for identification of underutilized land in Europe. *Rem. Sens., 13*, 4920. https://doi.org/10.3390/rs13234920

Spracklen, B. D., & Spracklen, D. V. (2019). Identifying European old-growth forests using remote sensing: A study in the Ukrainian Carpathians. *Forests, 10*, 127. https://doi.org/10.3390/f10020127

Strunk, J. L., Reutebuch, S. E., McGaughey, R. J., & Andersen, H.-E. (2025). An examination of GNSS positioning under dense conifer forest canopy in the Pacific Northwest, USA. *Remote Sensing Applications: Society and Environment, 37*, Article 101428. https://doi.org/10.1016/j.rsase.2024.101428

Valbuena, R., Mauro, F., Rodriguez-Solano, R., & Manzanera, J. A. (2010). Accuracy and precision of GPS receivers under forest canopies in a mountainous environment. *Spanish Journal of Agricultural Research, 8*, 1047–1057. https://doi.org/10.5424/sjar/2010084-1242

Vandekerkhove, K., Meyer, P., Kirchmeir, H., Piovesan, G., Hirschmugl, M., Larrieu, L., Kozak, D., Mikolas, M., Nagel, T., Schmitt, C., & Blumröder, J., 2022. Old-growth criteria and indicators for beech forests (Fageta) (No. LIFE-PROGNOSES-Work Package 1.11).

Vandekerkhove, K., Vanhellemont, M., Vrška, T., Meyer, P., Tabaku, V., Thomaes, A., Leyman, A., De Keersmaeker, L., & Verheyen, K. (2018). Very large trees in a lowland old-growth beech (Fagus sylvatica L.) forest: Density, size, growth and spatial patterns in comparison to reference sites in Europe. *Forest Ecology and Management, 417*, 1–17. https://doi.org/10.1016/j.foreco.2018.02.033

Vanhellemont, M. (2025). Life prognoses : WP1 & WP 2 : Methods & Site Description. *Instituut voor Natuur- en Bosonderzoek*. 10.21436/inbor.121256273.

Wing, B. M., Ritchie, M. W., Boston, K., Cohen, W. B., & Olsen, M. J. (2015). Individual snag detection using neighborhood attribute filtered airborne lidar data. *Remote Sensing of Environment, 163*, 165–179. https://doi.org/10.1016/j.rse.2015.03.013

Wirth, C., Messier, C., Bergeron, Y., Frank, D., & Fankhänel, A. (2009). Old-growth forest definitions: A pragmatic view. In: Old-Growth Forests. Springer Berlin Heidelberg (pp. 11–33). doi:10.1007/978-3-540-92706-8_2.

Xu, Y., & Goodacre, R. (2018). On splitting training and validation set: A comparative study of cross-validation, bootstrap and systematic sampling for estimating the generalization performance of supervised learning. *Journal of Analysis and Testing, 2*, 249–262. https://doi.org/10.1007/s41664-018-0068-2

Ziaco, E., Di Filippo, A., Alessandrini, A., Baliva, M., D'andrea, E., & Piovesan, G. (2012). Old-growth attributes in a network of Apennines (Italy) beech forests: Disentangling the role of past human interferences and biogeoclimate. *Plant Biosystems - An International Journal Dealing with all Aspects of Plant Biology, 146*, 153–166.